DEVELOPING METANET-BASED MACRO TRAFFIC MODEL FOR DHAKA CITY WITH MODIFIED LINK-SPECIFIC AND GLOBAL DRIVER PARAMETERS

SANJANA HOSSAIN

DEPARTMENT OF CIVIL ENGINEERING
BANGLADESH UNIVERSITY OF ENGINEERING AND TECHNOLOGY (BUET)
Dhaka, Bangladesh

November, 2015

DEVELOPING METANET-BASED MACRO TRAFFIC MODEL FOR DHAKA CITY WITH MODIFIED LINK-SPECIFIC AND GLOBAL DRIVER PARAMETERS

A THESIS SUBMITTED TO THE DEPARTMENT OF CIVIL ENGINEERING IN PARTIAL FULFILLMENT OF THE REQUIREMENTS FOR THE DEGREE OF

MASTERS OF SCIENCE IN CIVIL ENGINEERING
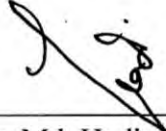
(CIVIL AND TRANSPORTATION)

SUBMITTED BY

SANJANA HOSSAIN
DEPARTMENT OF CIVIL ENGINEERING
BANGLADESH UNIVERSITY OF ENGINEERING AND TECHNOLOGY (BUET)
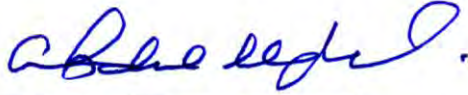Dhaka, Bangladesh

November, 2015

The thesis titled "**DEVELOPING METANET-BASED MACRO TRAFFIC MODEL FOR DHAKA CITY WITH MODIFIED LINK-SPECIFIC AND GLOBAL DRIVER PARAMETERS**" submitted by Sanjana Hossain, Student number – 0413042442 P and session April, 2013 has been accepted as satisfactory in partial fulfillment of the requirement for the degree of **Masters of Science in Civil Engineering (Civil and Transportation)** on 11th November, 2015.

Board of Examiners

(1) Dr. Md. Hadiuzzaman
Assistant Professor,
Department of Civil Engineering,
BUET, Dhaka-1000.

Chairman
(Supervisor)

(2) Dr. Abdul Muqtadir
Professor and Head,
Department of Civil Engineering,
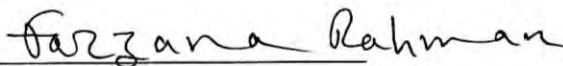BUET, Dhaka-1000.

Member
(Ex-officio)

(3) Dr. Tanweer Hasan
Professor,
Department of Civil Engineering,
BUET, Dhaka-1000.

Member

(4) Dr. Md. Mizanur Rahman
Professor,
Department of Civil Engineering,
BUET, Dhaka-1000.

Member

(5) Dr. Farzana Rahman
Associate Professor,
Department of Civil Engineering,
UAP, Dhaka-1205.

Member
(External)

i

DECLARATION

It is hereby declared that the work presented in this thesis has been done by the author and that full or part of this thesis has not been submitted elsewhere for the award of any degree or diploma.

November, 2015

Sanjana Hossain
Student No. 0413042442 P

ABSTRACT

Classical traffic flow models cannot be readily applied in heterogeneous traffic systems owing to the complex nature of their traffic dynamics. This paper develops a stochastic macroscopic model for traffic state estimation and short-term prediction in such systems. The proposed model takes into account the wide variation in the operating and performance characteristics of vehicles in heterogeneous condition through the use of variable fundamental diagrams (FDs) for different links. The model also allows for the underestimation of flow and speed due to the effect of vehicular influence area in the stated traffic condition. For this, normally distributed stochastic state influencing terms are used with the basic state estimation equations. In addition, an empirical parameter is introduced in the speed dynamics of the model to capture the sensitivity of traffic speed to the speeds of multiple leaders in a heterogeneous mix.

To confirm the structure of the FD, initially the speed-density plots of the field data for different links are fitted with four general structures: namely, the linear, logarithmic, exponential and polynomial forms. It is revealed that the 3rd degree polynomial structure is best suited for prevailing traffic condition. The optimized link-specific parameters of the model comply with those obtained from the regression analysis. Field validation with high-resolution traffic data proved that the proposed model can capture traffic dynamics quite accurately. To determine the individual contributions of the proposed model features, different structural variations of the final model are also investigated. It is revealed that the link-specific FD parameters and the stochastic traffic state influencing terms improve the model performance the most, followed by the empirical car-following parameter. Finally, compatibility analysis is performed on the proposed macroscopic model and a microscopic simulation model, VISSIM, to evaluate the performance of the macro model under varying traffic demand levels. Based on the performance of the two models, it is found that the prediction of traffic states from the macroscopic model is generally consistent with that from VISSIM simulation.

ACKNOWLEDGEMENTS

Table of Contents

List of Figures

List of Tables

Chapter 1

INTRODUCTION

1.1. Background of the study

In recent years, rapid increase in travel demand and the number of vehicles on roadways has resulted in serious traffic congestion problem for Dhaka city. According to a study jointly conducted by the Metropolitan Chamber of Commerce and Industry (MCCI) and Chartered Institute of Logistics and Transport Bangladesh in 2010, it was revealed that the annual cost of traffic congestion in capital Dhaka was around Tk 1 billion a day. The study found that about 3.2 million business hours were lost every day due to the traffic jams. A more recent assessment concluded that the estimated loss is now 50% more than what it was in 2010, adding up to a staggering amount of about Tk 550 billion annually. The traffic jams not only cause tremendous time and monetary losses but also compromise road safety and increase air pollution.

The most widely used strategy to mitigate the congestion problem is to increase roadway capacity by constructing new lanes. However, the growing demand issue cannot be mitigated by only expanding road infrastructure due to constraints like available right-of-way, capital investment, implementation time and environmental concern. Rather, more efficient use of the existing traffic network through Active Traffic Management (ATM) can be a better measure against the congestion problem at the short term. ATM involves the use of appropriate traffic flow models to accurately simulate and predict traffic state variables in real-time and then apply proper control strategy. In the developed countries, ATM has been successfully practiced for decades as a highly effective tool for mitigating traffic congestion and improving safety. Given the extent of the traffic jam problem in Dhaka, it is high time that the authority starts adopting ATM as a congestion mitigating tool. In this context, the development of a suitable macroscopic traffic flow model would be the first step in managing and controlling traffic flow and improving the overall mobility of the Dhaka city traffic.

Macroscopic traffic flow models play an irreplaceable role in real-time traffic state estimation and short-term prediction. The models consider the traffic flow as a compressible fluid and represent the traffic states with the help of aggregated variables: flow, speed and density. As such, they include a lower number of parameters compared to the microscopic models. This results in low computational effort and relative ease of calibration for real-time application. On the contrary, the microscopic models include a large number of physical or non-physical parameters that should be appropriately specified to reproduce the traffic flow characteristics with the highest possible accuracy. The parameter estimation has intensive computational requirements and is difficult to validate because human behaviour in real traffic is difficult to observe and model. Thus, macroscopic traffic flow models are generally preferred over microscopic models for real-time traffic estimation and control.

The two most frequently used macroscopic models are the first-order cell transmission model (CTM) (Daganzo, 1994) and the second-order METANET model (Messmer & Papageorgiou, 1990). Numerous studies like Lin & Ahanotu (1995), Muñoz et al. (2006), Papageorgiou et al. (1990) etc. have found that traffic state estimates of these models show very close agreement with the field data. Over the years, different extensions and modifications of these models have been proposed to adapt for a variety of traffic engineering tasks, such as dynamic traffic assignment, estimation and prediction, control strategy design and synthesis etc. For example, the CTM has been extended in Li (2010), Gomes & Horowitz (2006) and Hadiuzzaman & Qiu (2013) for arterial traffic signal control, freeways with ramp metering control and Variable Speed Limit (VSL) control respectively. Likewise, many extensions of the METANET model can be found in the literature to take into account e.g., weaving effect (Yin, 2014) and lane drops (Papageorgiou et al., 1990); and have been adapted to different models of ATM: variable speed limits (Islam et at., 2013), ramp meter control (Papamichail et al., 2010) and combination of these two (Lu et al., 2011).

These models were mostly developed and validated for homogeneous traffic. However, in Dhaka city, both motorized and non-motorized vehicles of different sizes, shapes and speeds ply over the roads making the traffic operating condition highly heterogeneous. Although recently, non-motorized traffic has been banned from the major roads of the city, the fact remains that here the traffic stream comprises of cars, buses, mini-buses, trucks, covered vans, auto-rickshaws and utilities having varying operating characteristics. The behaviour of traffic in such heterogeneous operating condition is significantly different from that in homogeneous condition. This necessitates the development of a new macroscopic model which will be able to successfully estimate and predict the heterogeneous traffic conditions of Dhaka city.

1.2 Statement of the problem and opportunities

1.2.1 Absence of appropriate high-resolution data collection technique

Within the vast literature on macroscopic traffic flow modeling, surprisingly few studies have addressed the heterogeneous traffic condition prevalent in many developing countries like Bangladesh, India etc. Such limited research is primarily attributed to the difficulty of high-resolution data collection in the stated traffic condition. Here loop detectors are unsuitable due to measurement errors caused by non-lane-based movement of vehicles activating either both or neither of two adjacent detectors. Moreover, traffic cameras for vehicle detection are often absent along the corridors. But given that accurate high-resolution traffic data is the pre-requisite for developing a successful traffic flow model, this research attempts to establish a data collection technique based on image processing which will be able to measure traffic states in the non-lane-based heterogeneous operating condition with reasonable accuracy. Also, the developed technique is expected to be robust and easy-to-use.

1.2.2 Unobserved nature of fundamental diagram

Although the conservation equation used in the macroscopic models is an exact equation, the description of mean speed is essentially empirical and is derived based on a static flow-density or speed-density relationship – the Fundamental Diagram (FD). It is generally recognized that FD is dependent on flow conditions and roadway environments. Consequently, various structures of the FD have been adopted in different models to capture the intrinsic functional relationship for the whole range of traffic situations; from free flow to congested equilibrium states including non-equilibrium transitions between them. For instance, the FD corresponding to the flow-density relationship in the original CTM (Daganzo, 1994) was assumed to be trapezoidal shaped, but it was further adapted to accommodate any continuous, piecewise differentiable FDs, such as a triangular FD. The METANET assumed an exponential speed-density relationship which was extended to explain the impact of the VSL, ramp metering etc. on traffic flow. These structures of the FD were found to reproduce the relevant traffic conditions for homogeneous traffic scenario with remarkable accuracy. However, due to different microscopic characteristics of vehicles in heterogeneous traffic compared to the homogenous condition, the aggregated macroscopic behaviour is likely to be different. This necessitates extensive investigation of FD structures for understanding flow transition phenomenon under the non-lane-based heterogeneous traffic conditions. Unfortunately, very few field studies have been undertaken for this investigation and so there remains much scope of research in this area.

1.2.3 Modification of macroscopic model for heterogeneous traffic

The core of ATM is the macroscopic traffic models for traffic state prediction. The accuracy of traffic state estimation and prediction affects the control decisions that will be assigned for mitigating the congestion problem. Unfortunately, no such model has been developed till date for simulating the non-lane-based heterogeneous traffic conditions of Dhaka city. Hence, as a stepping stone for ATM implementation, an appropriate macroscopic model should be developed for the stated traffic condition by proposing necessary modifications to state-of-art traffic flow models. The modified model should be able to successfully reproduce the wide variation in operating and performance characteristics of vehicles in heterogeneous traffic systems. More specifically, it should be able to capture the rapid change of traffic states along the roadway in the heterogeneous condition. Previous studies (Lu et al., 2011) showed that the speed dynamics of macroscopic simulation models like the METANET cannot catch quick and significant changes in congested traffic conditions. As a result, considerable prediction errors exist between the measured data and the model-predicted traffic states in such operating condition. Moreover, there remains some inherent differences between lane-based and non-lane based operations which affect the overall mobility of the traffic stream. Therefore, these problems should be investigated thoroughly to improve the sensitivity of the model performance under various traffic conditions.

1.2.4 Compatibility between microscopic and macroscopic simulation models

Now-a-days both microscopic and macroscopic simulations are widely used in transportation studies. Microscopic simulations are often used to explicitly capture interactions among individual drivers and represent the driver's response to traffic control devices at the individual vehicle level. However, this type of application is usually off-line and lacks predictive control functions. On the other hand, the application of macroscopic simulation models is aimed at large-scale roadway networks or online (real time) traffic control to reduce congestion and improve mobility.

Due to traffic operation safety and cost constraints, it is not practical, sometimes even impossible, to carry out experiments of various control measures on freeways. Traffic simulation is often used for experimental investigation purposes. The effects of a control strategy are often evaluated prior to the field implementation of online traffic control using microscopic simulations to determine whether the control strategy will have the expected performance. In this way, the optimal control policy for various traffic conditions can be determined based on several experimental settings and then used in actual field traffic control. Thus it is required to check whether both macroscopic and microscopic models provide similar traffic state results under all traffic conditions, including light traffic, moderate traffic, heavy traffic and excessively congested traffic. This issue is investigated in the present thesis.

1.3 Research objectives and scope of work

The goal of this study is to improve the overall mobility of Dhaka city's traffic. With this end in view, the research aims at developing a stochastic macroscopic model that will address the problems as mentioned in Section 1.2. The main objectives of this research work are listed below.

(1) To introduce a ready-for-practice method using image processing technique that can provide accurate high resolution traffic data for non-lane-based heterogeneous traffic conditions.

(2) To investigate the nature of fundamental diagram (FD) for understanding flow transition phenomenon under the non-lane-based heterogeneous traffic conditions.

(3) To establish METANET-based speed dynamics capable of reproducing the impacts of variable FDs and presence of multiple leaders in non-lane-based heterogeneous operating conditions so that the overall traffic state prediction accuracy is increased.

(4) To explore the compatibility of the developed macroscopic model with microscopic model under various traffic conditions so as to determine the traffic demand impacts on macroscopic simulation performance.

The scope of this research is restricted to uninterrupted arterials (including on-ramps and off-ramps) having heterogeneous motorized traffic. The test site is the Tongi Diversion

Road, a section of the Dhaka-Mymensingh Highway (N3) in Bangladesh (shown in Figure 1.1). It is an 8-lane major artery road in Dhaka, which connects the capital city with the Shahjalal International Airport. The developed model is expected to accurately estimate and predict the complex nature of the prevailing heterogeneous traffic condition of the test site through appropriate modifications and extensions of conventional traffic models.

Although arterial roads with signal controls are not included in the study, the methodologies and principles used here can be extended and applied to other types of roadways. The research is carried out using both simulations and field data obtained from the studied roadway section. The main test site is illustrated in Figure 1.1 and the research flow chart is shown in Figure 1.2.

1.4 Organization of the thesis

This thesis consisting of six chapters is structured as follows:

Chapter 1 gives an introduction of the relevant research background, statement of problems as well as the objectives and scope of this research.

Chapter 2 comprehensively reviews previous works on traffic flow models with a special focus on microscopic car-following models as well as first-order and second-order macroscopic models. The traffic models are reviewed with respect to their categories in terms of level of detail, scale of independent variables and nature of independent variables.

Chapter 3 presents details of the study site selected and the high-resolution data collection and processing techniques adopted for the research. Some justifications regarding the choice of methods employed are also provided.

Chapter 4 proposes a stochastic second-order macroscopic model for the heterogeneous traffic condition of Dhaka city. For this, it first investigates the nature of the traffic flow and the structures of the FD of different links of the study section utilizing the collected field data. Based on the results of this investigation and other empirical observations, the dynamics of the proposed model are described. Next, the model's global and link-specific parameters are determined through a least squares optimization problem using measured traffic data. Then the developed model is validated using another set of field data to accurately simulate the traffic system. Finally, different structural variations of the model are analyzed to determine the individual contributions of the proposed model features.

Chapter 5 studies the compatibility between the developed macroscopic model and a microscopic simulation model, VISSIM, to evaluate how the change in traffic demand impacts the macroscopic simulation performance. The predicted flow, density and speed from the models are compared for four levels of traffic demands for this purpose.

Chapter 6 summarizes the main conclusions of this research and discusses recommendations for future research works related to macroscopic traffic flow models and simulation for heterogeneous traffic.
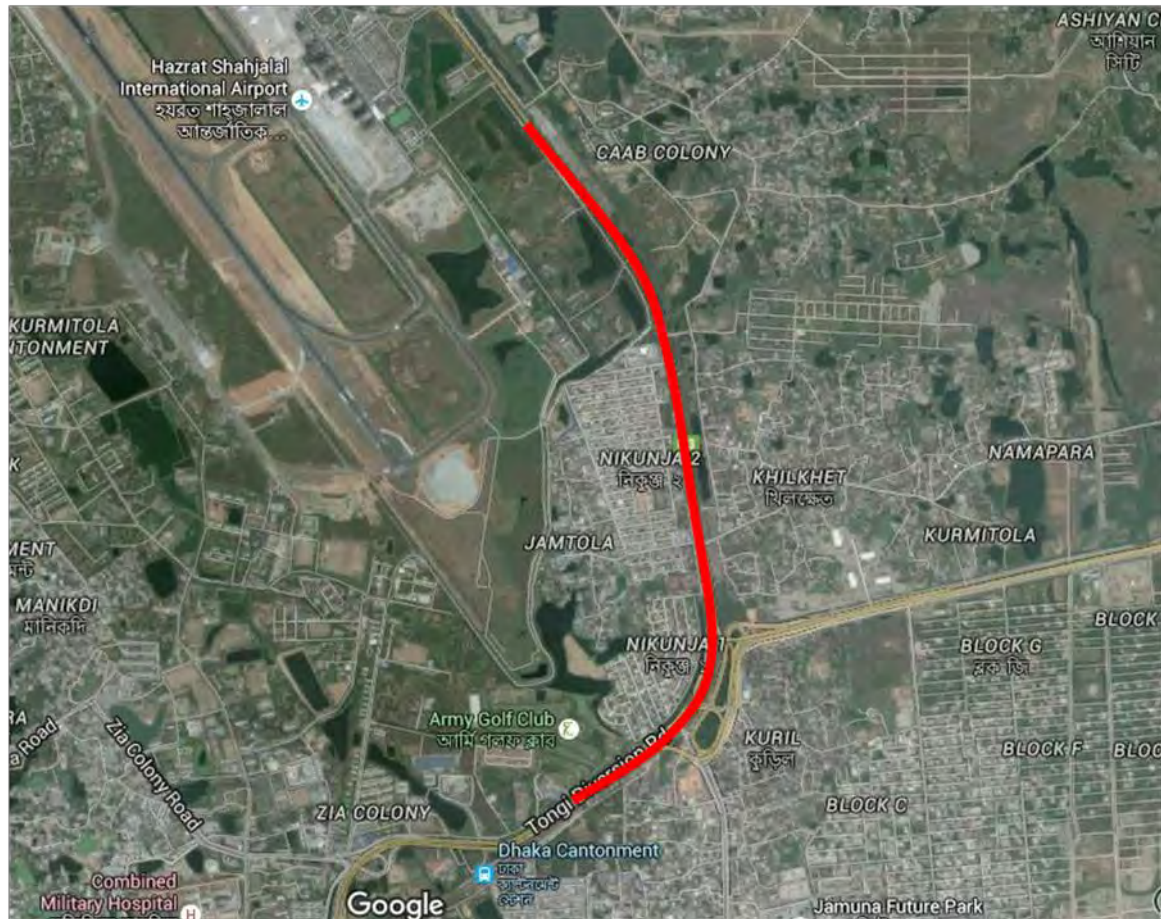
Figure 1.1 The 3.26 km long study site between Armed Forces Medical College and CAAB Head Quarters (courtesy: Google maps). Details can be found in Figure 3.1.

Traffic Operation Research

Video-based Data Collection

Image Processing
(Background Subtraction Technique)

Field Traffic States
(Measured speed & flow;
estimated density)

FD investigation through regression analysis
and identifying the most suitable structure

Investigation of the nature of heterogeneous traffic operation

Review of existing macroscopic models

Selection of base model (the METANET)

Proposed modifications:
(1) Introducing stochastic state influencing terms
(2) Using link-specific polynomial structured FD
(3) Introduction of a car-following parameter in the anticipation term of speed dynamics

A stochastic second-order macroscopic model for heterogeneous traffic

Model Derivation

Defining Objective Function

Constraints on Traffic Dynamics

Initial conditions and Boundary conditions

Problem Formulation

Gradient-based Optimization
(SQP)

Optimization Method

Macroscopic Simulation
(within MATLAB)

Compatibility analysis

Microscopic Simulation
(Field Data-based VISSIM model)

Performance Evaluation

Figure 1.2 Flow chart of the research

7

Chapter 2

LITERATURE REVIEW

Research on traffic flow models started from the mid-1950s, when the propagation of shock waves was modelled by Lighthill & Whitham (1955) and Richards (1956) based on the analogy of vehicles in traffic flow and particles in a fluid. Since then, numerous modeling approaches have been studied, from simple one-regime linear speed-density relationships to multi-regime, multi-class, nonlinear models. This chapter presents a historical overview of a rich variety of modelling approaches developed so far and in use today. Here, theoretical issues of model derivation and characteristics and some practical issues, such as model calibration and validation, will be discussed.

2.1 Categorization of traffic flow models

Traffic flow models may be categorized according to various criteria, such as the level of detail represented in the model, the scale of independent variables, the nature of variables used in modelling, operationalization criterion of the models, their scale of application etc. These classes are discussed briefly in the following sub-sections.

2.1.1 Level of detail

Traffic models are generally classified into four categories according to the level of detail with which they represent the traffic systems. These are:

(a) Sub-microscopic models: These are highly detailed descriptions of the functioning of vehicle motions, where even the behaviour of specific vehicles' subunits and the interaction with their surroundings are considered. For example, detailed description of driving behaviour, vehicle control behaviour (e.g. changing gears, AICC operation, etc.) in correspondence to prevailing surrounding conditions are modelled with precision here.

(b) Microscopic models: These models take each individual vehicle as a unit and track its motion and interaction with adjacent vehicles in the traffic stream. They operate based on the properties of each vehicle and on a set of rules. Typical examples of this kind of model are the car-following models for longitudinal movement and the lane-changing models for lateral movement on multi-lane roadways, on-ramps and off-ramps.

(c) Mesoscopic models: These are medium-detailed models where small groups of interacting vehicles are traced, instead of individual vehicle units. Behavioural information can be incorporated by means of probabilistic terms.

(d) Macroscopic models: These models are low-detailed representations of traffic states using aggregated variables, such as flow, average speed and density. They describe the collective effect of many vehicles. Individual vehicle motions and interactions are

completely neglected. These models are often derived from the analogy between vehicular flow and the flow of continuous media (e.g. fluids or gases).

Detailed description of sub-microscopic and mesoscopic models are not included hereafter, since they are out of the scope of this research. However, a comprehensive review on all these types of traffic flow models can be found in Hoogendoorn and Bovy (2001).

2.1.2 Scale of the independent variables

According to the scale of independent variables, traffic flow models can be classified as either continuous models or discrete models.

(a) **Continuous models:** The independent variables of these models change continuously and instantaneously both in time and space in response to continuous stimuli. These models are often formulated as differential equations in which time and space are treated as continuous variables over the study domain. Most of the car-following models are examples of this approach and so are hydro-dynamic macroscopic models.

(b) **Discrete models:** These models assume discontinuous changes in both time and space. Accordingly, traffic states are described temporally and spatially at discrete steps along the roadway. Examples of such discrete models include the cellular automata model (CA), the cell transmission model (CTM) etc.

2.1.3 Nature of the independent variables

According to the nature of independent variables used for representing the operation processes, traffic flow models can be distinguished as deterministic and stochastic models.

(a) **Deterministic models:** In these models all the factors are defined by exact relationships, i.e. there are no randomized components of these models. As such, if a traffic situation is simulated twice using a deterministic model, starting from the same initial conditions and with the same inputs and boundary conditions, the outputs of both simulations are the same. The METANET model, discussed in Chapter 4, is an example of a deterministic traffic model.

(b) **Stochastic models:** Stochastic model descriptions use random variables and a probabilistic approach to describe traffic states. This implies that two simulations of the same model starting from the same initial conditions, the same boundary conditions and the same inputs may return different results, depending on the value of the stochastic variable during each simulation. A stochastic variable can be characterized by its distribution function or by its histogram. For example, in the microscopic simulation package Paramics, a distribution of the level of patience over different drivers needs to be defined. During simulation, this distribution is sampled to determine an individual level of patience for every driver simulated in the network. A second simulation, and thus a new sampling of the distribution, will result in

drivers with other levels of patience. Therefore, stochastic models need to be simulated repeatedly and the results need to be averaged in order to be able to draw conclusions. Stochastic variables are used to model stochastic processes present in real-life traffic situations.

2.2 Microscopic traffic flow models

As mentioned earlier, microscopic traffic models describe the space–time behaviour of the systems' entities (i.e. vehicles and drivers) as well as their interactions at a high level of detail (individually). In other words, these models simulate the longitudinal (car-following) and lateral (lane-changing) behaviour of individual vehicles in relation to the roadway and other vehicles in the traffic flow. From this point of view, the microscopic traffic flow models are broadly classified into two categories: (i) the car-following and (ii) the lane-changing models. Both of these types are reviewed in detail in the following sub-sections.

2.2.1 Car-following models

Car-following models are a major part of this microscopic model category. They describe the processes by which drivers follow each other in the traffic stream. Research efforts were focused on the development of such *follow-the-leader models* from the 1960s when Pipes (1953) proposed an expression for the position of the leader vehicle as a function of the position of its follower. Three categories of car-following models will be briefly reviewed here, namely safe-distance models, stimulus-response models and psycho-spacing models. Other types of car-following models include the intelligent driver models, optimum velocity models, fuzzy logic-based models etc. Extensive reviews of different types of car-following models can be found in established literatures like Brackstone and McDonald (1999) and Wilson and Ward (2011).

2.2.1.1 Safe-distance models

In safe-distance or collision avoidance models, the driver of the following vehicle is assumed to always keep a safe distance from the vehicle in front, so that a collision will never happen. The first and the simplest model of this category was given by Pipes (1953), where the minimum safe distance between the leader and the following vehicle was assumed to be a function of the speed of the following vehicle (in miles per hour [mph]) and the length of the vehicle (in feet [ft]) in front, as indicated in Equation (2.1).

$$D_n(v) = L_n\left(1 + \frac{v}{1.47 * 10}\right) \tag{2.1}$$

Here, $D_n(v)$ is the gross distance headway of the following vehicle n driving with velocity v with respect to the leading vehicle $n-1$ that must be maintained to avoid collision between them. L_n denotes the length of vehicle n and 1.47 is a conversion factor to convert from mph to ft/s. Thus Pipes model is a simple linear car-following

model which essentially states that that the minimum safe distance between two vehicles corresponds to one car length at a minimum, and that it increases by one car length for every 10-mile increment in the speed of the following vehicle. Forbes et al. (1958) proposed a similar model formulation based on the minimum time headway between two vehicles. This model assumed that the minimal time headway was equal to the class-specific reaction time and the time required for the vehicle to travel a distance equal to its length.

Kometani and Sasaki (1959) derived a car-following model from basic Newtonian equations of motion. They sought to specify a safe following distance within which a collision would be unavoidable, if the driver of the vehicle in front were to act ‗unpredictably‗. Effectively, their formulation included a time delay between a change in the behavior of a vehicle and the actual reaction of its follower to this change. The full original formulation is as follows:

$$\Delta x(t-\tau) = \alpha v_{n-1}^2(t-\tau) + \beta v_n^2(t) + \gamma v_n(t) + b_0 \tag{2.2}$$

Where τ is the time delay; α, β, γ and b_0 are constants (model parameters) that need to be determined in model calibration. Data for calibration were generated by a pair of test vehicles driving on a city street, and collected using a cine film camera at the top of a roadside building. The observed road section covered almost 200 m with an average speeds of <45 kmph. A total of 22 test runs were conducted which deduced about 310 seconds of data for analysis, with a resolution of 1/8 s. The best fit to the above relationship, which was quite sharply peaked at an r^2 of 0.75, occurred for the following parameter set:

$$\Delta x(t-0.5) = -0.00028 v_{n-1}^2(t-0.5) + 0.00028 v_n^2(t) + 0.585 v_n(t) + 4.1$$

Thus the Kometani and Sasaki model is a nonlinear regression model with parameters related to the speed of the pair of vehicles.

Gipps (1981) refined safe-distance car-following models by assuming that ‗the driver travels as fast as safety and the limitations of the vehicle permit‗:

$$v_n(t+\tau) = \min \left\{ \begin{array}{l} v_n(t) + 2.5 a_{max} \tau \left(1 - \dfrac{v_n(t)}{v_{max}}\right) \sqrt{0.25 - \dfrac{v_n(t)}{v_{max}}}, \\[2em] a_{min}\tau + \sqrt{a_{min}^2 \tau^2 - a_{min}\left(2\left(x_{n-1}(t) - x_n(t) - s_{jam}\right) - v_n(t)\tau - \dfrac{v_{n-1}(t)^2}{b}\right)} \end{array} \right\} \tag{2.3}$$

with a_{max} maximum acceleration, a_{min} maximum deceleration (minimum acceleration), v_{max} the desired (maximum) velocity and s_{jam} jam spacing. s_{jam} is the jam spacing which is the front-to-front distance between two vehicles at standstill. Effectively, Gipps‗ approach introduced two regimes: one in which the vehicle itself limits its velocity [the

top part in Equation (2.3)], and one in which the safe distance to the leader limits velocity (the bottom part in the equation).

Leutzbach (1988) discussed a more refined model describing the spacing of constrained vehicles in the traffic flow. He states that the overall reaction time T consists of:

   a) perception time (time needed by the driver to recognize that there is an obstacle),
   b) decision time (time needed to make a decision to decelerate) and
   c) braking time (time needed to apply the brakes).

The total safety distance model assumes that drivers consider braking distances large enough to permit them to brake to a stop without causing a rear-end collision with the preceding vehicles if the latter vehicles come to a stop instantaneously. The corresponding safe distance headway equals:

$$D_n(v) = L_n + Tv + \frac{v^2}{2\mu g} \tag{2.4}$$

Here, μ is the weight of friction of the vehicle with road surface and g is the acceleration due to gravity.

2.2.1.2 Stimulus-response models

The second branch of car-following models discussed in this research consists of stimulus–response models. The car-following process of these models is based on the following basic principle:

Response (t+τ) = Sensitivity x Stimulus (t)

A stimulus at time t together with the driver's sensitivity causes a driver reaction after a reaction time τ. The stimulus is usually represented by the relative velocity (speed difference) of the leading and the following vehicle or the spacing between the two vehicles. The response is represented by the acceleration or deceleration of the following vehicle.

During the late 1950s and early 1960s there was a rapid development of the stimulus-response models. The first model of this category was proposed by Chandler et al. (1958). They assumed that the sensitivity term was a constant and the response was in the form of:

$$a_n(t+\tau) = \gamma \left[v_{n-1}(t) - v_n(t) \right] \tag{2.5}$$

Where, $v_n(t)$ and $a_n(t)$ denote velocity and acceleration respectively of vehicle n at t and γ is the sensitivity of the following vehicle that needs to be determined in experiments or model calibration. This model is a linear model with speed difference as the stimulus.

Subsequent researches on stimulus-response models were aimed at improving the description of the sensitivity of the following vehicle. This included using different sensitivity factors for acceleration and deceleration (as in Herman and Rothery, 1965 and Newell, 1965), introducing the distance between two vehicles (as in the third model proposed by the General Motors (GM) research team) and the speed of the following vehicle (as in the fourth GM car-following model).

All these efforts behind improving the stimulus-response models are consolidated in the now famous Gazis-Herman-Rothery (GHR) model, named after Gazis et al. (1961). This model considers exponents of both speed and distance in the sensitivity term thus improving the overall accuracy of the model.

$$a_n(t+\tau) = \frac{\alpha_{l,m}\left[v_n(t+\tau)\right]^m}{\left[x_{n-1}(t)-x_n(t)\right]^l}\left[v_{n-1}(t)-v_n(t)\right] \qquad (2.6)$$

Where, x_{n-1} and v_{n-1} represent position and speed of the leading vehicle, respectively, and x_n, v_n and a_n represent position, speed and acceleration of the following vehicle, respectively. m is the speed exponent, l is the distance headway exponent and $\alpha_{l,m}$ is a model constant. By assuming different values of m and l, several special cases of car-following models can be obtained.

However, the GHR model simulates the behaviour of free-flowing drivers very unrealistically. For example, the model assumes that the follower reacts to the actions of the leader, even though the distance to the leader is very large, and that the follower's response disappears as soon as the relative speed is zero. Also, according to the model, slow drivers are dragged along when following faster vehicles. This is obviously different from real-world traffic. These shortcomings can be corrected by either extending the GHR-model with additional regimes, e.g., free driving, emergency deceleration, etc., or by using a psycho-physical model or fuzzy logic-based models.

Some of the most popular more recent stimulus–response models include the optimal velocity model with delay by Bando et al. (1998), the two-regime intelligent driver model by Treiber et al. (2010), the acceleration delay model by Kerner and Klenov (2006), the stochastic car-following model by Kerner and Klenov (2002) etc.

2.2.1.3 Psycho-spacing models

This approach to car-following modelling is based on behavioural thresholds referred to as action points and was first proposed by Michaels (1963). It remedies the problems of stimulus-response models identified in the previous section by using insights from perceptual driver psychology. The idea is that drivers are subject to certain limits in their perception of the stimuli to which they respond (Todosiev and Barbosa, 1964). It is thus possible to identify space-time thresholds that trigger different acceleration profile

characterizations of a driver. Drivers will react to changes in speed difference or spacing only when these thresholds are reached (Leutzbach, 1988).

The basic behavioural rules of such so-called psycho-spacing models are:

1. At large spacings, the following driver is not influenced by velocity differences.
2. At small spacings, some combinations of relative velocities and distance headways do not yield a response of the following driver, because the relative motion is too small.

The most famous psycho-spacing model was developed by Wiedemann (1974). He distinguished constrained and unconstrained driving by considering perception thresholds. This car-following model utilizes these perception thresholds to describe the longitudinal motion of individual vehicles. The main concept of the model is that the follower starts to adjust its speed by applying continuous deceleration as it reaches its own perception threshold to a slower lead vehicle. However, since it cannot exactly determine the speed of the lead vehicle, the follower's speed will drop below the lead vehicle's speed until the follower applies slight acceleration after reaching another perception threshold. This results in an iterative process of acceleration and deceleration.

There are four different stages of following a lead vehicle (PTV 2012):

1. Free driving: In this mode, there is no influence of the lead vehicle. The follower travels at its desired speed.
2. Approaching: In this mode, the follower tries to adapt to the lead vehicle's speed. The follower applies a continuous deceleration so that the speed difference between them is zero when it reaches its desired safety distance.
3. Following: In this mode, two close vehicles maintain a safe distance, and their relative speed fluctuates around zero. The follower maintains its speed close to the lead vehicle without any conscious acceleration or deceleration.
4. Braking: In this mode, the relative distance between vehicles falls below a safe distance. This could be a result of a sudden deceleration of the lead vehicle; a third vehicle merges in front of the follower, etc.

Other noteworthy psycho-spacing models include the models of Lee & Jones (1967) [which uses spacing-based threshold for driver perception], Evans and Rothery (1973) [which quantifies Michaels' (1963) thresholds through a series of perception-based experiments], Krauss et al. (1999) [which addresses transient traffic flow behaviour, like the capacity drop, and stability of so-called wide jams] etc.

Psycho-spacing models are the foundation of a number of contemporary microscopic simulation models. For example, the microscopic simulation package, VISSIM (PTV 2012) which is described in detail in Chapter 5, uses the psycho-physical driver behaviour model proposed by Wiedemann (1974).

2.2.2 Lane-changing models

Lane changing refers to the lateral movements of vehicles from one lane to another. It may happen mandatorily at merge and diverge areas, or voluntarily at multi-lane roadways. Near on-ramp or lane-drop areas, merging maneuvers are one of the direct causes for the overloading of certain lanes and may lead to traffic breakdown (Cassidy and Bertini, 1999). In addition, voluntary lane changing can be the origin of perturbations that may lead to jams in dense and unstable traffic. As such, most models classify lane changes as either mandatory or discretionary lane change. Although lane-changing models are not as widely studied as car-following models, it is essential to incorporate this mechanism in traffic flow models. Extensive review on lane-changing models can be found in Moridpour et al. (2006) and Toledo (2007).

Moridpour et al. (2006) classified the different approaches taken in lane changing studies from the point of view of either driving assistance or driving decision systems. They defined driving assistance models as the models which consider the steering wheel angle and lateral motions to control the lane changing performance of vehicles. They further subdivided this category into collision prevention models and automation models. Collision prevention lane changing models are developed to control drivers' lane changing manoeuvres and assist them to execute a safe lane change. The collision prevention models are intended to improve road safety. Automation models are applied to perform the driving tasks either partially or entirely. The models of Lygeros et al. (1998), Eidehall et al. (2007), Kiefer and Hankey (2008), Li-sheng et al. (2009) etc. include such automotive adjustments to the steering wheel angle of vehicles to control their lateral motion and reduce dangerous lane changing manoeuvres.

Moridpour et al.'s other category of lane changing models focuses on drivers' lane changing decisions under different traffic conditions and under different situational and environmental characteristics. They classified drivers' decisions while responding to the surrounding environment, as either strategic, tactical or operational (Sukthankar et al. 1997). This classification is based on the time required for executing the decisions. The strategic level is the highest decision level and deals with drivers' decisions which require over 30 seconds making and executing. A driver's destination choice, mode choice and route choice are examples of strategic driving decisions (Alexiadis et al. 2004). While executing the strategic level decisions, a series of tactical decisions are made by the drivers, such as a decision to pass a slow moving vehicle or maintaining the desired speed. At the tactical, or intermediate, decision level, the time required for making and executing the decisions is between 5 and 30 seconds (Alexiadis et al. 2004). At the lowest decision level or the operational level, drivers decide about the manoeuvres to control their vehicles. These take place on a time scale of less than five seconds and include decisions such as whether or not to accept a gap (Alexiadis et al. 2004).

A famous lane-change model is the one by Wiedemann (1974), the principle of which is that drivers try to avoid discomfort in their own lane (for example, the vehicle in front is too slow compared with their desired speed) and seek the speed advantage of other lanes.

This desire for lane change leads to a lane change manoeuvre, if the gap in the target lane is sufficient to perform a safe manoeuvre.

Different from car-following, in the lane-changing model, the drivers' behaviour in the presence of interacting vehicular flows cannot be described as a function of the state of the leading vehicle, but must also take into account the distance and speed of the back and front vehicles on the target lane. Considering lane changing in microscopic models allows for the realization of necessary (mandatory) lane changes at on-ramps or lane closures as well as discretionary lane changes in preparation for passing slower vehicles.

2.2.3 Commercial microscopic simulation models

With the increased availability of fast computers in recent years, the application of microscopic simulation as a tool to reflect real-world traffic systems is gaining popularity. The number of traffic simulation models has increased significantly and by the end of the last century, there were more than 70 simulation models available according a study by U.C. Berkley (Skabardonis, 1999). Detailed review on such simulation models can be found in established literatures like Algers et al. (1997), Gao (2008), Olstam & Tapani (2004) etc. Among the large amount of traffic simulation models, five well-known models are the CORSIM, the AIMSUN, the VISSIM, the PARAMICS, and the INTEGRATION microscopic traffic simulation models. Each traffic simulation model has its unique underlying logic. The car-following and lane-changing logics used in each of these five models are listed in Table 2.1 below.

Table 2.1 Car-following and lane-changing logics of different microscopic simulation models

Microscopic Traffic Simulation Software	Car-following logic	Lane-changing logic
AIMSUN (Advanced Interactive Microscopic Simulator for Urban and NonUrban Networks)	Gipps (1981) safety-distance model	Gipps (1986) lane-changing model
PARAMICS	Psycho-physical model of Fritzche (1994)	Gap-acceptance model
CORSIM (CORidor SIMulation)	NETSIM for arterials with at-grade intersection and FRESIM for uninterrupted facilities.	Gipps (1986) lane-changing model which considers both mandatory and discretionary lane changes
INTEGRATION	Car-following models of Van Aerde (1995) and Van Aerde & Rakha (1995)	Considers both mandatory and discretionary lane changes
VISSIM	Psycho-physical models of Wiedemann (1974) for urban traffic and Wiedemann (1999) for motorway	Lane-changing model of Willmann and Sparmann (1978)

2.3 Macroscopic traffic flow models

The macroscopic approach of traffic flow modeling represents the traffic states with the help of aggregated variables and yields flow models with a limited number of equations. Most of the macroscopic models suggested so far are derived from the microscopic car-following considerations within a string of identical vehicles. However, the car-following models are only empirical and multilane traffic flow includes different types of vehicles and driving behaviours. Based on these facts, Papageorgiou (1998) convincingly argues that the deduced macroscopic model structures are unlikely to be as accurate as Newtonian physics or thermo-dynamics; rather their accuracy must be triggered via parameter calibration using real data.

Two basic equations always hold in all of the macroscopic traffic flow models. One is the conservation equation, which states that the change in number of vehicles on the roadway segment *(x, x + dx)* during time interval *(t, t+dt)* is equal to the number of vehicles flowing into that segment minus the number of vehicles flowing out of that segment. That is, vehicles are neither automatically generated nor taken away on an enclosed section of roadway. This is expressed as a partial differential equation (Gartner el al. 2001):

$$\frac{\partial \rho}{\partial t} + \frac{\partial q}{\partial x} = g(x,t) \tag{2.7}$$

Or as in an integration form:

$$\frac{\partial}{\partial t} \int_{x1}^{x_2} \rho(x,t)dx = q(x_1,t) - q(x_2,t) + g(x,t) \tag{2.8}$$

Where, q stands for flow, ρ for density and v for space-mean-speed. g is the generation rate within the road segment (from on-ramps and off-ramps), x and t stands for space and time, respectively.

Another equation is the basic traffic flow equation, namely, flow equals to the density times the space-mean-speed.

$$q = v.\rho \tag{2.9}$$

Equations (2.7) and (2.9) form a system of two independent equations with three unknown variables ρ, v and q. To solve this system, another independent equation is required. The different formulations of the third equation resulted in a series of macroscopic models. In this section, we discuss the two major types of macroscopic traffic models, namely, the first-order traffic models and the second-order traffic models.

2.3.1 First-order macroscopic traffic models

The most widely used first-order macroscopic traffic model was developed by Lighthill and Whitham (1955), and Richards (1956) independently (LWR model), which is a

continuous macroscopic representation of traffic variables. In the LWR model, the speed and/or flow rate are considered as a function of density:

$$v(x,t) = V_e \left[\rho(x,t) \right] \tag{2.10}$$

Hence,

$$q(x,t) = q_e \left[\rho(x,t) \right] = \rho(x,t) . V_e \left[\rho(x,t) \right] \tag{2.11}$$

Where, V_e denotes the equilibrium speed. It is a monotonically decreasing function of density. The relationship between density $\rho(x, t)$ and flow $q(x, t)$ is called the fundamental diagram (FD). The flow function is convex with a downward concavity (LeVeque, 1992). Since Equation (2.11) does not specify the functional form of the FD, many specific functions have been proposed either from fitting the measured data or from analytical deliberations, or a combination of both.

The solution of the nonlinear Equations (2.7), (2.9) and (2.10) is of the general form as in Equation (2.12) (Gazis 1967), which means that all points are on a straight line with slope v having the same density:

$$\rho(x,t) = F(x - v.t) \tag{2.12}$$

Where, F is an arbitrary function. Equation (2.17) implies that inhomogeneity, such as changes in density of vehicles, propagates along a stream of traffic at a constant speed $V_w = \partial q / \partial \rho$, which is positive or negative with respect to a stationary observer, depending on whether the density is below or above the optimum density corresponding to maximum q (Figure 2.2). The shockwave speed is expressed in Equation (2.13) and shown in Figure 2.2.

$$V_w = \frac{q_b - q_a}{\rho_b - \rho_a} \tag{2.13}$$
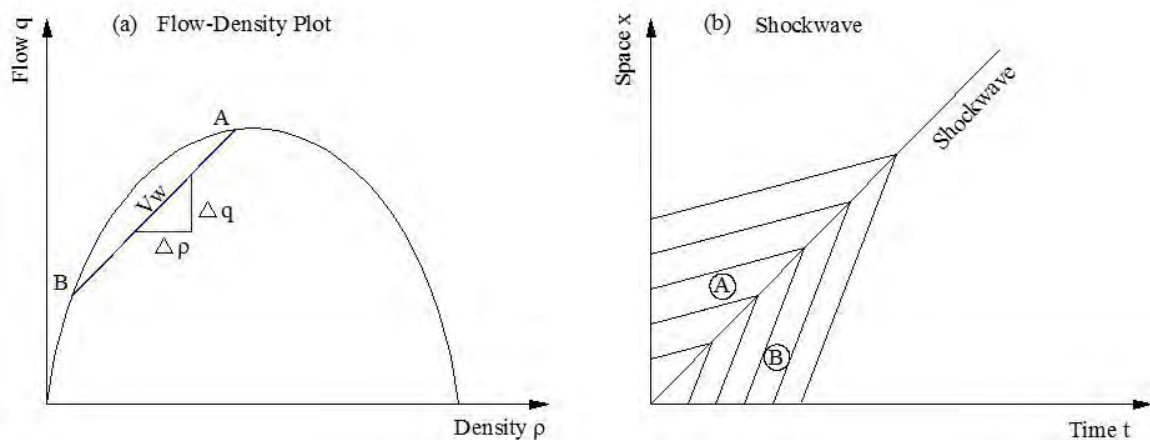
Figure 2.1 Shock wave formations resulting from the solution of the conservation

Most of the first-order macroscopic traffic flow models are discretized derivatives or extensions of the LWR model. Within this category, the cell transmission model (CTM) is the most popular, owing to its analytical simplicity and ability to reproduce congestion wave propagation dynamics. In this model, the roadway is discretized into small segments (cells) of uniform length. One cell may have at most one on-ramp and one off-ramp. The length of cells is set equivalent to the distance vehicles travel in one clock tick (time interval or time step) in light traffic (free flow). Under light traffic, all vehicles in a cell can be assumed to advance to the next cell in each time interval. The model functions based on the law of vehicle conservation: the number of vehicles in cell i at the next time step $(k+1)$ equals to the number of vehicles currently in cell i, plus the inflow from the upstream cell $(i-1)$ to cell i and minus the outflow to the downstream from cell i to cell $(i+1)$ between the time indexes k and $(k+1)$. That is:

$$n_i(k+1) = n_i(k) + y_{i-1}(k) + r_i(k) - y_i(k) - s_i(k) \tag{2.14}$$

Where, i is the cell index and k is the time index. $n_i(k)$ is the number of vehicles in cell i at time index k. $y_i(k)$ is the number of vehicles flowing out from cell i. $r_i(k)$ is the number of vehicles flowing into cell i from the on-ramp. $s_i(k)$ is the number of vehicles flowing out from cell i at the off-ramp.

The number of vehicles from one cell advancing to the next cell is controlled by boundary conditions, which guarantee the number of vehicles that can flow to downstream cells. CTM has three boundary conditions: at the upstream of the first cell, an adequate number of vehicles can flow into the first cell. Downstream of the last cell has sufficient capacity to allow vehicles to move away from the last cell. Between any pair of adjacent cells, the number of vehicles can flow to the next cell subject to the constraint:

$$y_i(k) = \min\left\{v_f \cdot \rho_c, Q_i, w_{i+1} \cdot (\rho_{\max} - \rho_c)\right\}$$

Where, v_f is the free flow speed, ρ_c, ρ_{max} are the critical and jam densities, respectively. w_{i+1} is the shockwave speed in the immediate downstream cell.

The average speed is determined by a steady-state speed-density FD, assuming all traffic speeds abide by this relationship at all traffic states. Originally, the FD corresponding to the speed-density relationship in CTM was assumed to be of trapezoidal shape, but it was further adapted to accommodate any continuous, piecewise differentiable FDs, such as a triangular fundamental diagram.

Dividing Equation (2.14) by the length of the cell, the density of the cells is obtained on both sides of the equation. Therefore, CTM is essentially a density dynamics model that evolves with boundary conditions.

Lin & Ahanotu (1995) compared the performance of the CTM under both congested and non-congested traffic conditions with data collected from a continuous segment of freeway I-880 in California. It was found that in free-flow condition, CTM provides as high as a 0.9 correlation value at a sampling interval of 6 seconds and asymptotically

tends to a perfect correlation at large sampling intervals. Again, a density-based modified version (Muñoz et al., 2006) of the CTM produced density estimates which showed only 13% mean error (averaged over all the test days) with measured densities on I-210 West in Southern California during the morning rush-hour period. Further research by Daganzo (1995a), Daganzo et al. (1997) and Feldman & Maher (2002) had expanded on the CTM to model junctions, highway links with special lanes and signalised networks respectively.

First-order traffic models can capture most of the important traffic flow characteristics, such as formation and dissipation of shock waves. However, as noted by Zhang (1998), Gartner et al. (2001) and other related studies, the first-order models are unable to capture traffic instability, driver's delayed response to traffic conditions and their anticipation behaviour. To overcome these shortcomings and to improve the accuracy level provided by first-order models, second-order models were developed.

2.3.2 Second-order macroscopic traffic models

While the first-order macroscopic traffic models are characterized by a single dynamical partial differential equation for flow and density, and the speeds are derived from a static speed-density relationship, the second-order models have an independent speed dynamics in addition to density dynamics. Such a speed dynamics describes the local acceleration as a function of speed and/or density as well as other possible exogenous factors.

As early as the mid-1950s, Lighthill and Whitham (1955), in their seminal work on kinematic waves, suggested that higher order terms be added to account for some traffic properties, such as inertia and anticipation, and they proposed a general form of a motion equation:

$$\frac{\partial q}{\partial t} + c\frac{\partial q}{\partial x} + T\frac{\partial^2 q}{\partial t^2} - D\frac{\partial^2 q}{\partial x^2} = 0 \tag{2.15}$$

Where, c is the traffic wave speed, T is the inertia time constant for adjustment of speed, D is the coefficient of diffusion. The authors did not provide an independent speed dynamics for this model.

The most popular second-order model was suggested by Payne (1971), which has both speed and density dynamics. He showed that the average speed in a section of a roadway is influenced by three major mechanisms: relaxation, convection and anticipation. Payne approximated individual driver behaviour with the help of the following equation:

$$v\left[(t+\tau), x(x,t+\tau)\right] = V_e\left\{\rho\left[t, x(t) + \Delta x\right]\right\} \tag{2.16}$$

This equation expresses that the speed of an individual vehicle after a reaction time τ is equal to the equilibrium speed corresponding to the density some distance Δx downstream. After repeatedly applying linear Taylor approximations to Equation (2.22) and using the density at the midway of two vehicles to represent the space headway, the

following dynamic equation for the average speed was obtained:

$$\frac{\partial v(x,t)}{\partial t} + v(x,t)\frac{\partial v(x,t)}{\partial x} = \underbrace{\frac{V_e\big[\rho(x,t)\big] - v(x,t)}{\tau}}_{\text{relaxation}} - \underbrace{\frac{c_0^2(x,t)}{\rho(x,t)}\cdot\frac{\partial \rho(x,t)}{\partial x}}_{\text{anticipation}} \qquad (2.17)$$

$$\underbrace{\qquad\qquad\qquad}_{\text{convection}}$$

$$c_0^2(x,t) = -\frac{1}{\tau}\frac{dV_e\big[\rho(x,t)\big]}{d\rho} \qquad (2.18)$$

Where c_o is the anticipation factor. Payne defined the three different terms of Equation 2.17 as:

- **Convection:** It accounts for the change in average speed at a location due to vehicles leaving or arriving with different speeds

- **Relaxation:** It describes the tendency of traffic flow to relax to an equilibrium speed, which corresponds to the homogeneous steady state in the flow. It is assumed that an equilibrium speed $V_e(\rho)$ exists, but the traffic state can deviate from it. When other influences (reflected by the convection and anticipation terms) are small, traffic tends to relax to the equilibrium speed.

- **Anticipation:** It describes driver's anticipation on spatially changing traffic conditions (reflected by the spatial variation of density) downstream.

Discretisation and modifications of the Payne model have led to the origin of a family of second-order models like the models of Payne (1979), Papageorgiou (1990), Lyrintzis et al. (1994) and Liu et al. (1998). Among these, the most widely used is the METANET model, which was validated against real traffic data with remarkable accuracy at several instances. For example, Papageorgiou et al. (1990) successfully estimated the traffic states of a 6-km stretch of the southern part of Boulevard Périphérique in Paris with standard deviations of only 10.8 km/h for mean speeds and 714 veh/h for traffic volumes. But it was noted that the same parameter values of the exponential FD were used for all links in spite of the different shapes appearing from the field data at different sites. Sanwal et al. (1996) extended the METANET to model the flow under the influence of traffic-obstructing incidents. The extended model, when fitted to a 5.8 mile segment of the I-880 freeway between the Marina and Whipple exits in California, indicated quite satisfactory performance. Since the METANET contains both speed and density dynamics, it was successfully used as a candidate model for traffic control design in many studies, some of which are mentioned in the previous section. To avoid difficulty in control design and implementation, Lu et al. (2011) suggested a simplified version of the METANET, dropping the non-linear parameterization in the speed control variable. The simplified model with a modified convection term was able to estimate the field traffic dynamics more accurately than the original model.

Comparative evaluations of first and second-order models based on real data were reported by Cremer & Papageorgiou (1981), Michalopoulos et al. (1992), Spiliopoulou et al. (2014) etc. These studies provided empirical evidence of better accuracy of second-order models compared to first-order ones. But it should be noted that the second-order models also have weaknesses. Critical review by Daganzo (1995b) found logical flaws in the arguments that have been advanced to derive second order continuum models. In reaction to this criticism, Aw & Rascle (2000), Zhang (1998, 2002) and Liu et al. (1998) proposed variant models or improvements that avoid the identified flaws.

The second-order model derived by Aw and Rascle (2000) includes a density-dependent traffic pressure coefficient, and avoids the negative speed of Payne model, as criticized by Daganzo (1995b). The model can be written as:

$$\frac{\partial v}{\partial t} + v\frac{\partial v}{\partial x} = \frac{V_e(\rho) - v}{\tau} + \rho \cdot p'(\rho) \cdot \frac{\partial v}{\partial x} \tag{2.19}$$

Where, $p'(\rho)$ is the density-dependent traffic pressure coefficient. The acceleration equation of Zhang's (2002) model can be written as:

$$\frac{\partial v}{\partial t} + v\frac{\partial v}{\partial x} = \frac{V_e(\rho) - v}{\tau} - \frac{\left[\rho V'(\rho)\right]^2}{\rho}\rho_x \tag{2.20}$$

Where, $[\rho V'(\rho)]^2$ is the traffic sound speed. In this model, the traffic sound speed will never be faster than the actual traffic speed and, thus, avoids the back traveling problem, as in Payne's model, as criticized by Daganzo (1995).

Prigogine & Herman (1971) and Phillips (1979) proposed traffic models in which the continuity equation for the density and the acceleration equation were derived from kinetic principles. Since the density equation is based on conservation law, it is the same as in the first-order models. The acceleration equation is expressed as (Phillips 1979):

$$\frac{\partial v}{\partial t} + v\frac{\partial v}{\partial x} = \frac{V_e(\rho) - v}{\tau} - \frac{1}{\rho}\frac{\partial P_e}{\partial x} \tag{2.21}$$

Where, P_e is the ―traffic pressure.‖ This term was adopted from gas-kinetic considerations where the pressure term describes a purely kinematic (statistical) effect of speed variance without a single vehicle accelerating or braking. In traffic flow models, the pressure term is also referred to as the anticipation, which reflects the driver's anticipation to downstream traffic conditions and can be expressed as:

$$P_e = \rho \cdot \Theta_e = \upsilon \cdot \Theta_0 \left(1 - \frac{\rho}{\rho_{\max}}\right) \geq 0 \tag{2.22}$$

Where, Θ_e is the density dependent speed variance and Θ_0 is a positive constant (model parameter) that needs to be estimated. Kerner & Konhauser (1993) and Lee el al. (1998) introduced a viscous term into the acceleration equation for the purpose of smoothing

discontinuous traffic. The viscosity term is also called diffusion in macroscopic models (i.e., the second-order derivatives with respect to space). The intention of using this term is to smooth sharp transitions and shocks.

All above models account for the driver's delayed response (relaxation) and convection. The difference lies in the functional form of anticipation or traffic pressure and the viscous term. The models can be generalized as:

Vehicle Acceleration = Relaxation + Convection + Anticipation (or Pressure) + Diffusion (or Viscous term)

2.3.3 Traffic flow models for heterogeneous traffic

From the above discussions it becomes evident that the macroscopic traffic flow models are mostly empirical and they have their own pros and cons. Their performances may be very different for different operating conditions; viz. lane-based homogeneous, non-lane-based heterogeneous etc. Hence, Papageorgiou (1998) suggests that the sufficiency of the traffic flow theories be decided depending on the specific utilizations. Within the vast literature on macroscopic traffic flow modeling, surprisingly few studies have addressed the heterogeneous traffic condition prevalent in many developing countries like Bangladesh, India etc. Majority of these researches (e.g. Venkatesan et al. (2008), Arasan & Koshy (2005), Jin et al. (2010), Gunay (2007)) mainly focus on the microscopic approach of traffic flow modeling. Other works like (Chari & Badarinath, 1983 and Gupta & Khanna, 1986) focus on developing speed, flow and density relationships for mixed traffic conditions and introduce the concept of ―areal density‖ instead of linear density measurements.

A very limited number of first-order macroscopic models have also been developed for heterogeneous traffic. For instance, (Nair et al. 2011) views the disordered, heterogeneous traffic system as granular flow through a porous medium and extends the LWR theory using a new equilibrium speed-density relationship. This relationship explicitly considers the pore size distribution, enabling the model to successfully capture the ‗creeping‘ phenomena of heterogeneous queues. However, a microscopic simulation of vehicle configuration is used to determine the pore space distribution and detailed trajectory information of the disordered traffic stream is required for model calibration. Another extension (Wong & Wong, 2002) of the LWR model takes into account the dynamic behavior of heterogeneous users according to their choice of speeds in a traffic stream. The model uses an exponential form of speed-density relation and can replicate many puzzling traffic flow phenomena such as the two-capacity (or reverse-lambda) regimes occurred in the fundamental diagram, hysteresis and platoon dispersion. But being extended versions of the first-order LWR model, neither of these models have independent speed dynamics and they lack field validation.

2.4 Conclusion

This chapter provided an overview on the state-of-the-art of traffic flow models with a special focus on microscopic car-following models and second-order macroscopic models. The traffic models were reviewed with respect to their categories in terms of level of detail, scale of independent variables, nature of independent variables and model representations. Most of these models were developed and validated for lane-based car dominated operating condition. Only a very limited number of first-order macroscopic models for heterogeneous traffic were revealed from the extensive literature review. Hence, this research work aims at introducing a second-order flow model for heterogeneous traffic which is expected to show better accuracy in estimation of the complex traffic dynamics of Dhaka city.

Chapter 3
DATA COLLECTION AND PROCESSING

This chapter presents details of the study site selected and the high-resolution data collection and processing techniques adopted for the research. The collected data will serve as the basis for the development of the macroscopic and microscopic simulation models in the later part of this research. Some justification regarding the choice of methods employed are also provided here.

3.1 Study area

The study site is the Tongi Diversion Road, a section of the Dhaka-Mymensingh Highway (N3) in Bangladesh (shown in Figure 1.1). It is an 8-lane major artery road in Dhaka, which connects the capital city with the Shahjalal International Airport. The selected 3.26 kilometres (km) long uninterrupted section has one off-ramp, closely followed by an on-ramp. These form one diverge and one merge sections along the corridor. There are exactly 4 through lanes on each direction of the test site totaling up to a width of 14.48 metres (m) to 14.94 m in different links. The on and off ramps have two lanes each, though lane discipline is absent in the main stream flow and in the ramp flows. The test section experiences a directional average annual daily traffic (AADT) of about 11451 vehicles. The traffic stream consists of 40% cars, 12% microbuses or jeeps, 10% motorcycles, 8% buses, 10% utility vehicles and 20% auto-rickshaws. Such geometric and traffic characteristics make the test site an ideal study location for non-lane-based heterogeneous uninterrupted traffic condition.

3.2 Data collection

Collection of high-resolution traffic data required for the development of an accurate macroscopic model is a very challenging task under the existing traffic condition of the study area. This is mainly because loop detectors are unsuitable for the test site due to measurement errors caused by non-lane-based movement of vehicles activating either both or neither of two adjacent detectors. Moreover, traffic cameras for vehicle detection are absent along the corridor. Under these circumstances, video cameras are installed at various locations of the study site to provide traffic data for the research through image processing technique.

For macroscopic simulation, the corridor is discretized into five links with the lengths varying from 320 m to 920 m as shown in Figure 3.1. The off-ramp is located at the end of link 2 and the on-ramp is located at the beginning of link 3. Five video cameras are installed along the mainline, one at approximately mid-length of each link. The data obtained from each camera is considered representative of the traffic condition of the whole link. The ramps are also equipped with video cameras for collecting data of the merging and diverging traffic. The approximate locations of the cameras are also

indicated in Figure 3.1 whereas the details of each camera location can be found in Figure 3.2 (a-h).

Figure 3.1 Discretization details of the study area

Although the non-lane-based heterogeneous behaviour becomes more acute with the increase of traffic volume in the roadway, the test site was videoed from 3:00 PM to 6:00 PM covering both peak and off-peak periods for FD investigation. Two sets of videos were collected for the same time period on 15th and 16th April, 2015. These videos were processed and the extracted data was filtered for anomalies. Ultimately, 2.5 hours data of 15th April was used for calibration of the model parameters and the similar data set from 16th April was used for model validation. To ensure better quality of the collected data, the camera height and angle of projection were strictly maintained.

Figure 3.2 (a) Camera location on Link 1

Figure 3.2 (b) Camera location on Link 2

Figure 3.2 (c) Camera location on Link 3

Figure 3.2 (d) Camera location on Link 3 (close-up)

Figure 3.2 (e) Camera location on Link 4

Figure 3.2 (f) Camera location on Link 5
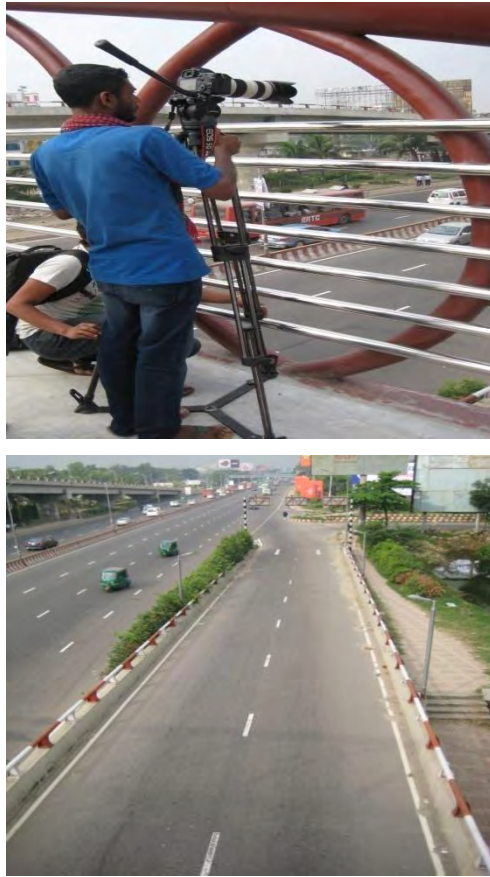
Figure 3.2 (g) Camera on off-ramp (above); Field of vision of the camera (below)

Figure 3.2 (h) Camera location on on-ramp showing details of the data collection process

As shown in Figure 3.2 (h), the mounting heights of the cameras were at least 20ft to reduce the object details detected by the image processing algorithm and the camera angle was less than 45 degrees to avoid perception problem. However, the angle was not so small as to cause restriction in vision. Due to the absence of suitable vantage points meeting such requirements in links 1, 2, 4 and the on-ramp location, cranes were used for mounting the cameras at the required height for a period of 3 consecutive hours each day. The presence of foot over bridges of sufficient height in links 3 and 5 and on the off-ramp location allowed the data collection process to be carried out without the use of cranes.

3.3 Data processing

For extracting high resolution traffic data from the video footages, an object detection algorithm has been used which operates based on the Background Subtraction (BGS) technique of image processing. The developed algorithm can successfully detect non-lane-based movement of vehicles. It can also identify non-motorized traffic, dark car and shadow quite accurately. Video data and vehicle geometry are provided as input to the algorithm and it gives vehicle count and time mean speed at required intervals as the output. For measuring flow, strip based counting method combining successive incremental differentiation is used. On the other hand, for measuring speed, the algorithm segments the whole field of vision and detects the change in center of area of an object in

28

each segment to find the corresponding pixel speed. Then calibrating the pixel distance with the field distance, instantaneous and time mean speeds are obtained, which can easily be converted to space mean speed. The density of the traffic stream for the research is estimated from the measured flow and speed.

The developed algorithm has been proved to give highly accurate traffic data with Mean Absolute Error (MAE) of only 14.01 and 0.88 in flow and speed measurements respectively when compared with actual field measurements. The algorithm addresses some of the major problems faced in the BGS technique, like the camouflage effect, camera jitter, sudden illumination variation, low camera angle and elevation etc. The process of traffic detection by the algorithm is briefly illustrated below.

3.3.1 Traffic detection technique

The background modeling algorithm used for traffic detection in this research is quite simple, yet accurate. It involves the use of static frames for object extraction from a video stream or image. Traffic is detected according to the following basic steps.

Step 1: Choosing the static background model (B)

This is the primary step of static background subtraction technique. The background model is a frame within the video having no traffic in it. This background is selected up careful inspection of the video. Figure 3.3 (a) shows such a background model used for traffic detection from the video of the off-ramp location of the study site.

Figure 3.3 (a) The background model (B)

Step 2: Selecting the frame (I) on which vehicle detection is to be performed

Using an iteration process, the frame on which the detection should be performed is to be selected one by one from the video file. Figure 3.3 (b) shows a typical frame for traffic detection.

Figure 3.3 (b) A random frame (I) for vehicle detection

Step 3: Determining the absolute difference (D) between B and I

The difference between the static background model B and the traffic detection frame I gives the differential image where only the traffic exists. For example, Figure 3.3 (c) is the differential image of the frame I of Figure 3.3 (b).

Figure 3.3 (c) The differential image (D) of frame I

Step 4: Converting differential image into binary image

In order to make the differential image machine readable, it is converted into binary image using a ―threshold value‖. The selection of proper threshold value is very important for accurate vehicle detection. In the differential image, the pixels having intensities lower than the selected threshold is assigned value ―0‖, whereas those having intensities higher than the threshold are assigned ―1‖. Thus the differential image gets converted into a binary code as in Figure 3.3 (d).

Figure 3.3 (d) The binary image of D

Step 5: Performing morphological operation

Next, some morphological operations are required for enhancing the quality of the binary image by removing unwanted ―noises". For this purpose, binary opening is used. Its magnitude depends on the type of opening algorithms used i.e. square, circular, disk type opening etc. On the other hand, binary closing is needed to recover an object from the binary image. Its magnitude depends on the same factors as opening. The improvement of the quality of binary image after applying opening and closing are shown in Figures 3.3 (e) and (f) respectively.
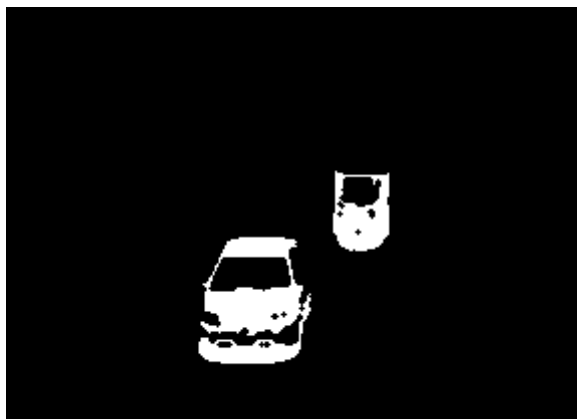
Figure 3.3 (e) Binary image after applying opening
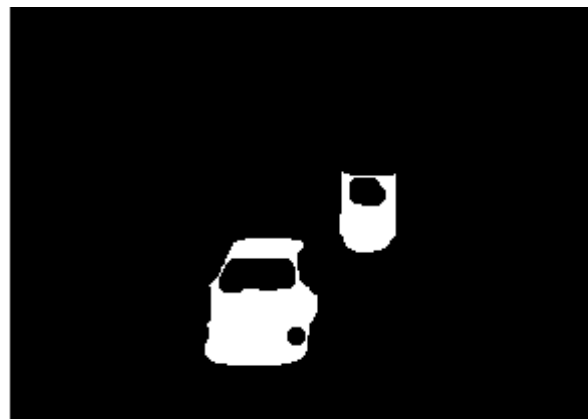
Figure 3.3 (f) Binary image after applying closing

Thus the vehicles from a video stream are extracted according to these steps, analyzing one frame at a time. Then applying the counting and speed measurement techniques mentioned earlier, the flow and speed data in the field condition are obtained at the required time interval (20 seconds for this research).

3.4 Conclusion

This research aims at developing a macroscopic flow model for the non-lane-based heterogeneous traffic condition of Dhaka city. For this high-resolution data is the pre-requisite. The current chapter introduced the test section used in this research along with details of the video-based data collection method adopted. It then briefly discussed the image processing technique used here for extracting flow and speed data from the video footages of the test site. The measured high-resolution data will be used for the development and analysis of the model in the subsequent chapters.

Chapter 4

MODEL DEVELOPMENT AND ANALYSIS

Macroscopic traffic flow models play a very important role in Active Traffic Management (ATM). They are used to accurately estimate and predict traffic state variables in real-time and then apply proper control strategy for mitigating anticipated traffic instabilities. Consequently, the underlying traffic flow model that is used for prediction within the ATM framework must capture all the relevant traffic dynamics, including free-flow and congestion states, and the transition between them. The present chapter focuses on the development of such a macroscopic model for the heterogeneous traffic condition of Dhaka city. For this, it first presents the details of the widely accepted second-order METANET model which will be used as the base model in this research. Then the nature of the traffic flow for heterogeneous operating condition is investigated utilizing the collected field data. Based on the results of this investigation and other empirical observations, a stochastic second-order traffic flow model is proposed which is then calibrated and validated to accurately simulate the traffic system. Finally, different structural variations of the final model are analyzed to determine the individual contributions of the proposed model features.

4.1 The METANET model

4.1.1 The basic METANET model

The following assumptions are used while describing the basic METANET model: a freeway section is divided into $i = (1, 2 \ldots N)$ links as in Figure 4.1 (the length of each link must be longer than the free-flow travel distance i.e., $v_{free}T \leq L_i$ to satisfy the *step size modeling constraint[1]*); a link contains exactly one on-ramp; a link may have multiple off-ramps; and each link contains at least one traffic sensor.
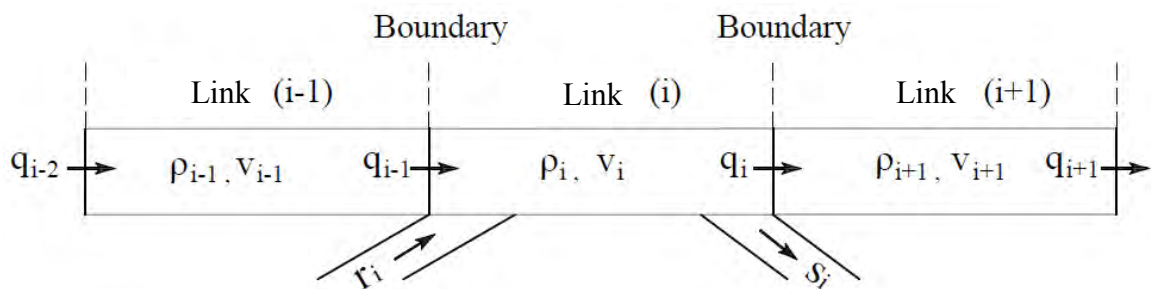
Figure 4.1 Discretization of a roadway section

---

[1] The relations of the (maximum) model time step, the maximum traffic speed and the minimum link length, in order to ensure that traffic doesn't travel more than one link during one time step.

In METANET, the density of a link is determined according to the flow conservation law; i.e., the density evolution of a link i at time step $k+1$ equals the previous density, plus, the inflow from the upstream link and on-ramp, minus the outflow of the link itself and off-ramp (Equation 4.1).

$$\rho_i(k+1) = \rho_i(k) + \frac{T}{L_i \lambda_i} \left[\lambda_{i-1} q_{i-1}(k) - \lambda_i q_i(k) + r_i(k) - s_i(k) \right] \tag{4.1}$$

The outflow (q_i) is equal to the link density multiplied by the space mean speed.

$$q_i(k) = \rho_i(k) v_i(k) \tag{4.2}$$

The on-ramp flow (r_i) takes the value of the minimum of three quantities, as in Equation 4.3: (1) the available traffic on the ramp; (2) the maximal flow allowed by the ramp; and (3) the admissible flow due to the mainline traffic conditions. The similar model is also used to compute the inflow (q_0) into the first link.

$$r_i(k) = \min \left[D_{ramp}(k) + \frac{\omega_{ramp}(k)}{T}, Q_{max,ramp}, Q_{max,ramp} \left(\frac{\rho_{jam,i} - \rho_i(k)}{\rho_{jam,i} - \rho_{c,i}(k)} \right) \right] \tag{4.3}$$

$$\omega_{ramp}(k) = \omega_{ramp}(k-1) + T \left(D_{ramp}(k-1) - r_i(k-1) \right) \tag{4.4}$$

In the above equation, $Q_{max,ramp}$ (vphpl), ρ_i (vpkpl), and $\rho_{jam,i}$ (vpkpl) represent, respectively, the capacity of the ramp, the density on the link i connected to the on-ramp, and the jam density of the link i connected to the given on-ramp.

The exit flow (s_i) from link i to the off-ramp is calculated using Equation (4.5):

$$s_i(k) = \frac{\phi_i(k)}{1 - \phi_i(k)} q_i(k) \tag{4.5}$$

The speed dynamics in METANET is equal to the summation of the previous speed, a relaxation term, a convection term and an anticipation term as in Equation (4.6). A brief illustration of these terms is presented below:

$$v_i(k+1) = v_i(k) + \underbrace{\frac{T}{\tau} \left[V[\rho_i(k)] - v_i(k) \right]}_{\text{Relaxation}} + \underbrace{\frac{T}{L_i} v_i(k) \left[v_{i-1}(k) - v_i(k) \right]}_{\text{Convection}} - \underbrace{\frac{1}{\tau} \left[\frac{T\upsilon}{L_i} \frac{\rho_{i+1}(k) - \rho_i(k)}{\rho_i(k) + \kappa} \right]}_{\text{Anticipation}} \tag{4.6}$$

Relaxation describes that the mean speed v of the link gets relaxed to the FD with a lag time τ.

Convection describes that vehicles entering from upstream link i-1 to current link i adapt their speed gradually rather than instantaneously.

Anticipation describes that drivers are looking ahead. If a driver sees high traffic density in the downstream link i+1, they will slow down, and vice-versa.

In Equation (4.6), the reaction time parameter – τ (hr), the anticipation parameter – υ (km²/hr), and the positive constant – κ (vpkpl) are the model's global parameters, i.e., all the links have the same value. These parameters are to be calibrated using the measured field data. In METANET, the above speed dynamics has been derived from Payne's model (Payne, 1971). However, the 4th term has been modified relative to Payne's model. Specifically, κ is added to avoid the singularity of the term when modeling low traffic density and υ is added to capture sensitivity of traffic speeds to the downstream traffic density.

The equilibrium speed $V[\rho_i(k)]$ (kph) of the FD in Equation (4.6) is represented by Equation (4.7):

$$V[\rho_i(k)] = v_{free} \exp\left[-\frac{1}{\alpha}\left(\frac{\rho_i(k)}{\rho_c}\right)^\alpha\right] \tag{4.7}$$

4.1.2 Some extensions of the basic METANET model

In some research, the speed dynamics i.e. Equation (4.6) was extended by including additional terms to directly account for the impacts from on-ramps, lane drops, weaving maneuvers or the blocking of lanes due to incidents. These terms may appear in different forms. For example, Cremer and May (1986), Papageorgiou et al. (1989) and Bellemans (2003) modeled the slow-down of traffic in the vicinity of an on-ramp (due to disturbances caused by the lane changing of the merging on-ramp traffic) by introducing an additional term having the following form:

$$\Delta v_{merge,i}(k) = -\frac{\delta_m T}{n_i L_i}\frac{r_i(k)v_i(k)}{\rho_i(k)+\kappa_m}$$

Where, δ_m is a tuning parameter for the merging term whose value depends upon the layout of the ramp and κ_m is a model constant. n_i is the number of merging lanes and r_i is the flow from the on-ramp. Yin (2014) proposed a slightly different form of the merging term to incorporate the speed of the on-ramps:

$$\Delta v_{merge,i}(k) = -\frac{\delta_m T}{n_i L_i}\frac{r_i(k)[v_i(k)-v_r(k)]}{\rho_i(k)+\kappa_m}$$

Where $v_r(k)$ is vehicle speed on on-ramp. When a lane is dropped ($\lambda_{i+1} < \lambda_i$), the effect on speed due to merging of traffic was modeled by Papageorgiou et al. (1990) through the addition of the following term to the right-hand side of Equation (4.6):

$$-\frac{\phi T}{L_i} \frac{(\lambda_i - \lambda_{i+1})}{\lambda_i} \frac{\rho_i(k)}{\rho_{cr}\lambda_i} v_i^2(k)$$

Here, ϕ is the constant parameter to account for the lane-drop effect. Another extension to the basic METANET model was proposed by Sanwal et al. (1996) to account for the blocking of one or more lanes of the highway during an incident:

$$-\frac{\phi_{lb}T}{L_i} \frac{[\lambda_i(k) - \lambda_{i+1}(k)]}{\lambda_i} \frac{\rho_i(k)}{\rho_{cr}\lambda_i} v_i^2(k)$$

The parameter ϕ_{lb} has been introduced for incident lane blocking. Again, Bellemans (2003) formulated an additional term of the speed dynamics to account for the impact of weaving, which can be re-written as:

$$\Delta v_{weaving,i}(k) = -\frac{\phi_w T}{n_i L_i} \frac{r_i(k)v_i(k)}{\rho_{cr}}$$

Here, ϕ_w is a tuning parameter. Yin (2014) proposed the following weaving term to include the volume of both entering and exiting traffic:

$$\Delta v_{weaving,i}(k) = -\frac{\phi_w T}{n_i L_i} \frac{[r_i(k) + s_i(k)]v_i(k)}{\rho_{cr}}$$

In this term, r_i and s_i are the in-flow from an on-ramp and the exit flow to an off-ramp respectively at the time step k. However, some research that included the on-ramp or lane-drop terms concluded that in many cases these extensions do not significantly improve the model accuracy. For example, Papageorgious et al. (1989) reported that including the on-ramp term in the model ―did not lead to any visible amelioration" whereas Papageorgiou et al. (1990) found that ―the importance of lane drop coefficient is moderate." Yin (2014) investigated different forms of merging and weaving terms and reached to similar conclusion. As such, the merge and lane-drop terms are not included in the scope of this research.

4.2 Investigating fundamental diagram for heterogeneous traffic

The fundamental diagram (describing flow-density, speed-density or speed-flow relationship at a given location or section of the roadway) is a basic tool in understanding the behavior of traffic stream characteristics in macroscopic flow models. In the 1st order models, speed is derived directly from a steady-state speed-density ($v - \rho$) FD; whereas in the Payne model and its derivatives, the speed dynamics generates a reference speed

based on the FD. Therefore, identifying the nature of this fundamental relationship is a prerequisite for the development of any macroscopic model. The current section aims at investigating the impact of the non-lane-based heterogeneous traffic condition on FD. More specifically, it will highlight on how the existing traffic characteristics of the test site influence the structure and parameters of the FD for the internal links L2, L3 and L4 which will be utilized for modeling purpose.

Over the years different structures of the FD have been proposed depending on the flow conditions and roadway environments. However, it is generally agreed that flow q is a concave function of density ρ defined in $[0, \rho_j]$ (ρ_j – jam density); and the corresponding v-ρ relationship is monotone decreasing. Since the FD will be used in the speed dynamics of the proposed model, only the v-ρ relationship is investigated in detail in this section. A few functional representations of this relation from the literature are given below.

Greenshields (1934) postulated a linear relationship between speed and traffic density based on the data obtained from a rural two-lane Ohio highway. The Greenberg model (1959) which is obtained by the integration of car-following model, proposed a logarithmic structure (Equation 4.8), observing speed-density data sets for tunnels. The Underwood model (1961) proposed an exponential v-ρ relationship (Equation 4.9) based on the results of traffic studies on the Merritt Parkway in Connecticut.

Greenberg model: $$v = V_m \ln\left(\frac{\rho}{\rho_j}\right) \tag{4.8}$$

Underwood model: $$v = V_f e^{-\frac{\rho}{\rho_c}} \tag{4.9}$$

Here, ρ_c, V_f and V_m represent critical density, free-flow speed and the speed corresponding to the maximum flow or ρ_c respectively. Edie (1961) suggested using a multi-regime model to represent the traffic breakdown near critical density ρ_c. He proposed the use of the Underwood model for the free-flow regime and the Greenberg model for the congested-flow regime, thereby overcoming the flaws of both of the models. Further developments in the field of FD were directed towards generalizing the modeling approach. Examples of such developments include the one-parameter polynomial model cited by Zhang (1999):

$$v = v_f\left(1 - \left(\frac{\rho}{\rho_j}\right)^n\right) \tag{4.10}$$

And the exponential model used in Papageorgiou et al. (1990), which is obtained by adding parameters for data fitting flexibility to the Underwood model:

$$V(\rho) = v_f \exp\left(-\frac{1}{\alpha}\left(\frac{\rho}{\rho_c}\right)^{\alpha}\right) \qquad (4.11)$$

To observe the nature of the fundamental relationship for heterogeneous traffic, the $v - \rho$ plots of the field data for different links are fitted with four general structures evident from the literature: namely, the linear, logarithmic, exponential and polynomial forms. Table 4.1 provides a comparative study among these structures, on the basis of their goodness-of-fit. The R-Squared and Root Mean Square Error (RMSE) values reveal that the 3rd degree polynomial relationship shows the best fit with the field data for all three links. In relation to the findings of Chari & Badarinath (1983), which deduced a logarithmic $v - \rho$ relationship with R-Square value of 0.41 utilizing time-lapse photographic data of Hyderabad, India, it can be said that the polynomial structure shows better fit for the prevailing traffic condition.

Table 4.1 Comparison of fitness of different structures of the fundamental diagram in heterogeneous traffic condition

Link No	Goodness-of-fit Parameters	Structure of the Fundamental Diagram (V vs. ρ)				
		$v = a_1\rho + a_2$	$v = a_1 \ln(a_2\rho)$	$v = a_1 \exp(a_2\rho)$	$v = a_1\rho^2 + a_2\rho + a_3$	$v = a_1\rho^3 + a_2\rho^2 + a_3\rho + a_4$
2	R-Square	0.5800	0.6451	0.6450	0.6364	0.6460
	RMSE	6.1171	5.6233	5.6243	5.6858	5.6254
3	R-Square	0.4909	0.5951	0.6014	0.5926	0.6036
	RMSE	3.7059	3.3014	3.2791	3.3116	3.2665
4	R-Square	0.6352	0.6882	0.6969	0.6971	0.7003
	RMSE	4.3238	3.9975	3.9411	3.9442	3.9276

Note: a_1, a_2, a_3, a_4 represent the estimated coefficients of the structures.

However, the polynomial type FD structure obtained above from the direct fitting of measured $v - \rho$ data is not readily used in the speed dynamics. This is because the FD parameters are not optimized in stand-alone mode in the model dynamics. Rather, all the global and link-specific parameters are optimized simultaneously. Thus to make the FD structure more generalized and to allow for data-fitting flexibility, Zhang's one-parameter polynomial structure (Equation 4.10) is used in the speed dynamics of the proposed model. An additional benefit of using this structure is that two important link-specific parameters v_f and ρ_j are obtained directly during model calibration. Nevertheless, the regression analysis provides important guidelines regarding the values of v_f and ρ_j for optimization of the whole model. Figure 4.2 (a-c) shows the speed vs density scatter plots of the links along with the best-fit regression lines.
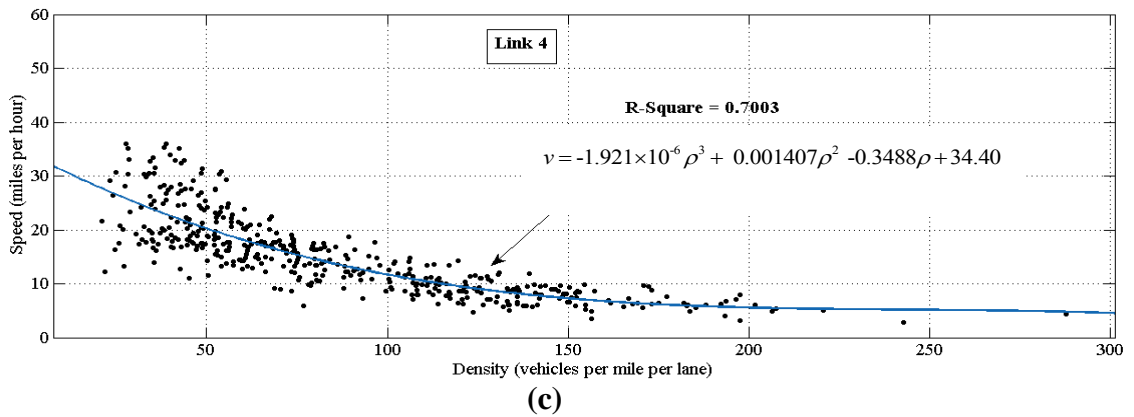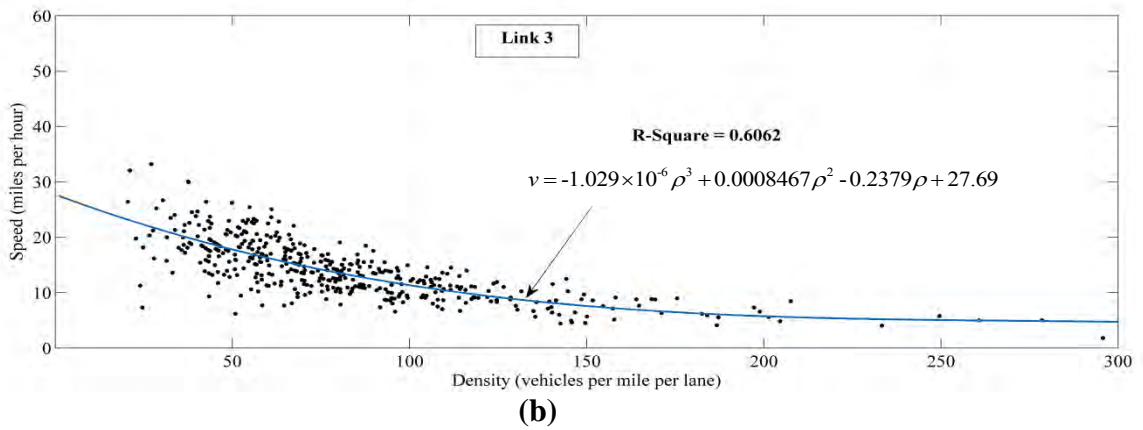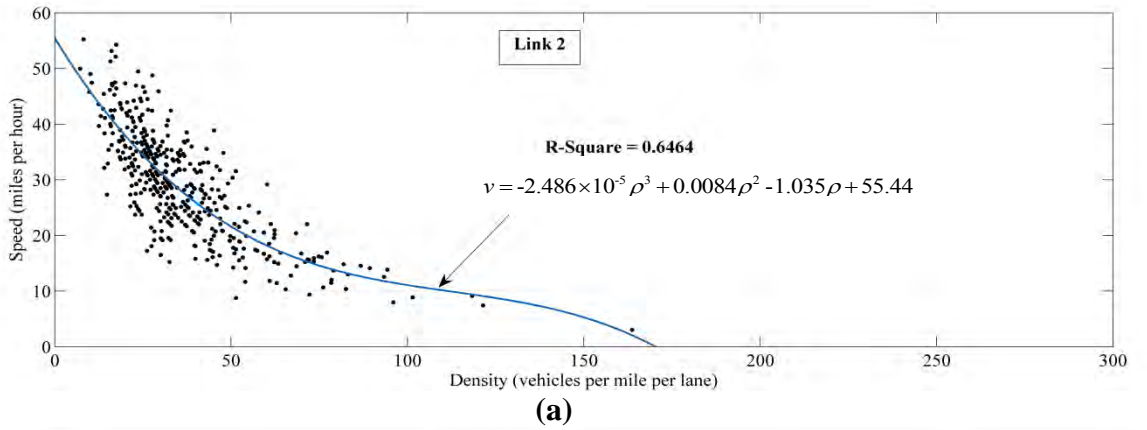
Figure 4.2 Speed vs. density scatter plots of links 2-4 (20 seconds resolution field data used in the plots was collected from 3:00 PM to 5:30 PM on 15th April, 2015.)

An in-depth investigation of the above plots reveals that the values of the FD parameters, i.e., v_j and ρ_j vary significantly for different links. In general, the links with greater roadside friction from pedestrian activities on raised sidewalk (as observed for L3 and L4) show lower free-flow speed and greater jam density compared to the link L2 with less roadside friction. This is because the presence of roadside friction causes sluggish transition from free flow state to congestion state. Thus, to capture the dynamics of heterogeneous traffic more accurately, the FD parameters are varied link-wise in the proposed model.

Other forms of FD can be very easily derived from the established v - ρ relationships. As

39

an example, the flow-density FD of link L2 is derived here. The v-ρ relationship of link L2 is represented by the following equation:

$$v = -2.486 \times 10^{-5} \rho^3 + 0.0084 \rho^2 - 1.035 \rho + 55.44 \qquad (4.12)$$

Multiplying both sides of this equation with ρ yields a functional form of the link's flow q. This is expressed as:

$$q = -2.486 \times 10^{-5} \rho^4 + 0.0084 \rho^3 - 1.035 \rho^2 + 55.44 \rho \qquad (4.13)$$

Differentiating both sides of Equation 4.13 with respect to ρ and then equating it with zero gives:

$$\frac{dq}{d\rho} = -9.944 \times 10^{-5} \rho^3 + 0.0252 \rho^2 - 2.07 \rho + 55.44 \qquad (4.14)$$

$$-9.944 \times 10^{-5} \rho^3 + 0.0252 \rho^2 - 2.07 \rho + 55.44 = 0 \qquad (4.15)$$

Solution of Equation 4.15 yields the density values for which the flow function's slope is zero. The solutions are $\rho = 66$, 75 and 112. Hence the critical density, ρ_c of link L2 is 112 vpmpl. Putting the value of ρ_c in Equation 4.13 gives the capacity of the link. The estimated capacity of the link is 1116 vphpl. Similarly, the FD parameters of the other links can also be determined. These are shown in Table 4.2

Table 4.2 Estimated FD parameters of different links

Link	Free flow speed v_f (mph)	Critical density ρ_c (vpmpl)	Jam density ρ_j (vpmpl)	Capacity q_{max} (vphpl)
L2	55.44	112	170	1116
L3	27.69	325	432	1456
L4	34.40	288	376	1371

An interesting observation from the table is that, while the values of ρ_c are quite large, the differences between ρ_c and ρ_j are relatively small. This implies that in heterogeneous operating condition, the critical density is reached rather slowly; but once the density of the roadway reaches this limit, relatively small increase in density causes stagnant congestion of the traffic stream, i.e. the operating speed falls to zero and the jam density is reached. Hence, for the heterogeneous traffic of the test site, the transition from the critical to jam densities is rather abrupt.

4.3 Traffic Dynamics

This section derives a stochastic METANET-based traffic flow model for the estimation and prediction of heterogeneous traffic states. The second-order macroscopic model is expected to depict the traffic dynamics more realistically than commonly used first-order

models, owing to its independent speed dynamics in addition to the density dynamics. Similar to the basic METANET model, the proposed model assumes discontinuous changes in both time and space. Thus, traffic states are described temporally and spatially at discrete steps along the roadway. The following assumptions are made in this respect: the roadway is divided into i (1, 2 ….N) links such that the length L_i of each link satisfies the step size modeling constraint i.e. $v_f T \leq L_i$; each link is a homogeneous unit containing exactly one on-ramp; a link may have multiple off-ramps; each link contains at least one traffic sensor (e.g. loop detector or video camera); and each link satisfies the equilibrium traffic state assumption individually. On the basis of these assumptions, the traffic dynamics of the proposed model are developed in the following sub-sections.

4.3.1 Density Dynamics

The density dynamics of the model is essentially the flow conservation law. Accordingly, the density evolution of the link i at time step $k+1$ equals the previous density, plus, the inflow from the upstream link and on-ramp, minus the outflow of the link itself and off-ramp (Equation 4.12).

$$\rho_i(k+1) = \rho_i(k) + \frac{T}{L_i \lambda_i}\left[\lambda_{i-1} q_{i-1}(k) - \lambda_i q_i(k) + r_i(k) - s_i(k)\right]$$

(4.12)

As in the base model, λ_i is the number of lanes of the link i. $r_i(k)$ and $s_i(k)$ are the on-ramp and off-ramp flows respectively. It is noted that Equation 4.12 is an exact equation and does not include any parameter to be calibrated.

4.3.2 Flow Estimation Equation

In most of the existing macroscopic models, the flow dynamics is expressed by the basic traffic flow equation, namely, flow equals density times space-mean-speed ($q = \rho * v$). This holds true for roadways with homogeneous traffic and strict lane discipline, where the movement of vehicles is essentially one-dimensional. Thus the dynamic characteristics of a vehicle in a lane affect the motion of its followers in that lane only (Figure 4.3 (left)). But in heterogeneous non-lane-based traffic movement, as Khan and Maini (1999) mentions, traffic does not move in single file. Rather, there is a significant amount of lateral movement. Since different classes of vehicles traverse in both the longitudinal and the lateral directions, they develop a critical ―influence area‖ around themselves as shown in Figure 4.3 (right). The nature of this influence area depends on a number of factors like, the speed of the vehicles, their sizes, acceleration and deceleration rates, maneuvering capacities and the behaviour of the drivers.
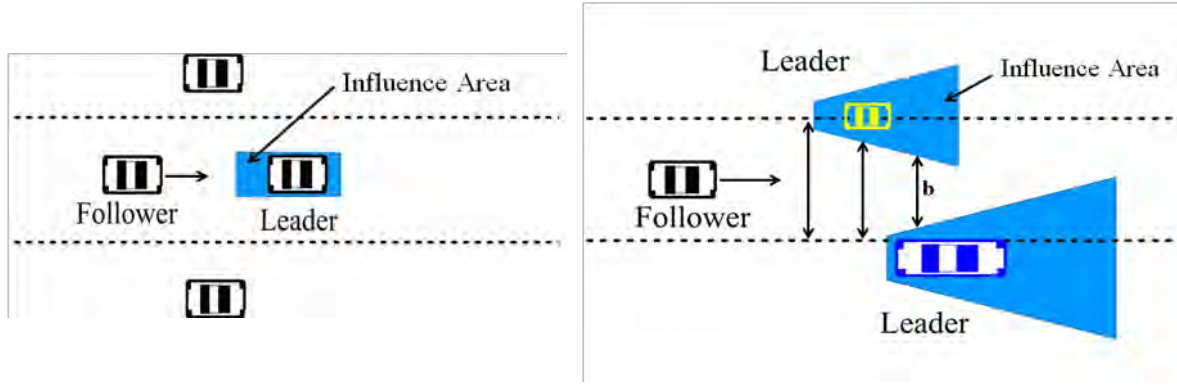
Figure 4.3 Lane-based homogeneous traffic (left) and non-lane-based heterogeneous traffic (right)

In general, traffic flow under heterogeneous condition is greater than the corresponding flow under homogeneous condition. This is because in the heterogeneous composition, the smaller vehicles occupy the gaps among the larger vehicles resulting in maximum space utilization. This space utilization is however constrained by the effect of influence area. If the available lateral clearance (denoted by _b' in Figure 4.3 (right)) among the influence areas of the leaders is greater than the minimum lateral clearance required for a particular class of vehicles to move, the vehicles will move forward in the traffic stream and vice-versa. In the lane-based operating condition, this available space remains constant for all classes of vehicles and is equal to the lane width of the roadway. As such, the flow computed by the basic traffic flow equation is accurate. However, in non-lane-based operating condition, the available lateral clearance varies according to the influence areas of the leaders, which again depends on a variety of static and dynamic properties of vehicles mentioned earlier. Thus, fundamental relation $q = \rho * v$ might underestimate the actual flow. The combined effect of optimum space utilization and vehicular influence area in non-lane-based heterogeneous traffic operation could vary significantly. However, it is hard to determine such effect accurately during real-time traffic state estimation. Thus, a stochastic flow influencing term $\xi_i^q \sim N(\mu, \sigma)$ is added to the flow equation to account for this underestimation. It is expected that the stochastic term could improve flow estimation significantly. The flow estimation equation of the proposed model is expressed as follows.

$$q_i(k) = \rho_i(k)v_i(k) + \xi_i^q(k) \tag{4.13}$$

4.3.3 Speed Dynamics

The speed dynamics of the original Payne model was derived from a linear car-following model that describes the behavior and interaction of the vehicles as they follow a leading vehicle on the road. It was shown that the speed of vehicles in a link is affected by (1) the density of vehicles in that link since the speed tends to relax to the equilibrium speed on FD, (2) the speed of (slower or faster) vehicles coming from the link upstream and (3) the perception of a relatively lower or higher density in the link downstream. In the speed dynamics, these three phenomena are expressed respectively by a relaxation term, a

convection term, and an anticipation term. The speed dynamics of the METANET model has been derived from Payne's model. However, the anticipation term has been modified relative to Payne's model. Specifically, κ, a positive constant is added to avoid the singularity of the term when modeling low traffic density and a global anticipation parameter, υ is added to capture sensitivity of traffic speeds to the downstream traffic density. It is worthwhile to mention here that, υ is added based on the heuristic microscopic considerations of Payne's model. Thus in lane-based homogeneous traffic, where a vehicle has only one leader, υ essentially captures the sensitivity of a driver's speed to the immediate downstream density in the same lane. However, in non-lane-based heterogeneous mix, a vehicle does not have one leader, but several, perhaps on the front-left, the front-straight, and the front-right (Figure 3b). Hence the speed of a vehicle is influenced by the speed of a number of surrounding leaders. To account for this, a dimensionless Car-Following (CF) parameter has been added to the anticipation term of the speed dynamics in the proposed model. This CF parameter, denoted by θ in Equation 4.14 is expected to capture the sensitivity of traffic speed to the speeds of the near-by vehicles. Similar to the flow dynamics, a stochastic speed influencing term $\xi_i^v \sim N(\mu, \sigma)$ is added to the empirical speed equation to reflect the impact of influence area on speed. Finally, the speed dynamics of the proposed model is expressed as in Equation 4.14 below.

$$v_i(k+1) = v_i(k) + \frac{T}{\tau}\Big[V\big[\rho_i(k)\big] - v_i(k)\Big] + \frac{T}{L_i}v_i(k)\big[v_{i-1}(k) - v_i(k)\big] - \frac{\theta}{\tau}\left[\frac{T\upsilon}{L_i}\frac{\rho_{i+1}(k) - \rho_i(k)}{\rho_i(k) + \kappa}\right] + \xi_i^v(k)$$

(4.14)

Here, τ is the reaction time parameter as in the Payne's model. According to the findings of the previous section, the FD $- V\big[\rho_i(k)\big]$ in Equation 4.14 is represented by Equation 4.15:

$$V\big[\rho_i(k)\big] = v_{f,i}\left(1 - \left(\frac{\rho_i(k)}{\rho_{j,i}}\right)^{n_i}\right)$$

(4.15)

where, v_j, ρ_j and n_i are respectively the free-flow speed, jam-density and shape parameter of the fundamental diagram for link i. The set of equations (4.12), (4.13), (4.14) and (4.15) constitutes the complete stochastic second-order model for heterogeneous traffic condition proposed in this study.

4.4 Model Calibration

The model parameters which need to be estimated are the global parameters τ, υ, κ and θ; the link-specific FD parameters v_j, ρ_j and n; the mean μ_i and standard deviation σ_i of the zero-mean Gaussian flow and speed influencing terms ξ_i^q and ξ_i^v introduced in the flow and speed dynamics respectively. During the calibration process, these parameters are chosen such that the objective function given in Equation 4.16 is minimized.

$$f = \sum_{i=1}^{N} \sum_{k=1}^{K} \left\{ \beta \left[\hat{q}_i(k) - \tilde{q}_i(k) \right]^2 + \gamma \left[\hat{v}_i(k) - \tilde{v}_i(k) \right]^2 + \left[\hat{\rho}_i(k) - \tilde{\rho}_i(k) \right]^2 \right\} \qquad (4.16)$$

Here, i is over all the links and k is the time step in the calibration time period. $\hat{q}_i(k), \hat{v}_i(k), \hat{\rho}_i(k)$ are the flow, speed, density collected from the field on 15th April, 2015, whereas $\tilde{q}_i(k), \tilde{v}_i(k), \tilde{\rho}_i(k)$ are the model estimated flow, speed, density. The weight factors β and γ are chosen so that the contributions of flow, speed and density errors are comparable. From the field data, it is found that the typical speeds, flows and densities are around 30 miles/hour (mph), 1250 vehicles/hour/lane (vphpl) and 40 vehicles/mile/lane (vpmpl). Accordingly, $\beta = (40/1250)^2 = 0.001$ and $\gamma = (40/30)^2 = 1.78$ are used in the optimization. Since the model is non-linear, f can have multiple local minima for a given convergence threshold. This research uses the gradient-based optimization method ―Sequential Quadratic Programming" (SQP) to minimize the objective function over a constrained parameter space. The algorithm starts with ten different initial estimates which satisfy a specified set of bounds for the acceptable values of the parameters. These points are then moved in the parameter space until the improvement in objective function reaches the predefined termination tolerance of 1×10^{-5}. The maximum number of iterations allowed for the evaluation of the function is set to be 3000.

During the parameter optimization, the sampling time T is taken to be 20 seconds which implies that the measured traffic data be aggregated into 20 seconds interval. Then, the total number of time steps, $K = (2.5 \text{ hours} \ast 3600 \text{ second} / 20 \text{ second}) = 450$ is assigned in Equation 4.16. The optimized parameter set is given in Table 4.3.

TABLE 4.3 Optimized parameter set of the proposed model

Link-specific Parameters							Global Parameters			
Link	v_f mph	ρ_j vpmpl	n	μ_v mph	σ_v mph	μ_q vph	σ_q vph	τ h	κ	υ m^2/h	θ
L2	50.35	200	3.504	0.387	1.532	281	7.992				
L3	24.5	291	3.275	0.675	2.297	992	8.845	0.0112	843021	584.553	53.0024
L4	31.8	241	3.136	1.871	12.73	448	2.639				

All the model parameters given in Table 4.3 are well optimized since none of these passes its assigned lower boundary or upper boundary values. Moreover, the trend and values of v_f and ρ_j of different links obtained from model optimization and direct regression analysis of the FD plots are in good agreement with each other. However, the values of ρ_j are slightly larger than the typical value of 200 vpmpl found in lane-based homogeneous traffic operation. This is representative of the existing heterogeneous traffic condition where space optimization by different classes of vehicles results in greater jam

densities than in the lane-based homogenous condition. The value of the CF parameter θ for this study is 53. If a driver in a traffic stream adjusts his speed following the speeds of a greater number of leaders, the value of θ will increase and vice versa.

4.5 Model Validation Results

In the words of Papageorgiou (1998), empirical validation remains the final criterion measuring the degree of accuracy, and hence the usefulness, of any macroscopic traffic flow model. Accordingly, in this section, the developed model is applied with the optimized parameter values to estimate traffic states and the results are compared with the set of measured traffic data collected on the 16th of April, 2015. Since the proposed model is supposed to describe traffic dynamics for the whole density range, the flow, speed and density at the boundary links, L1 and L5 are always assumed to be the measured field values. So, the traffic states of only the intermediate links L2, L3 and L4 are estimated by the model. Also, the ramp flows $r_i(k)$ and $s_i(k)$ of Equation 4.12 always take the measured values. The traffic states at the initial time step are assumed to be the measured field values for all the links. But after the first step, they are estimated by the model dynamics. The resulting speed, flow and density profiles for the intermediate links over the full simulation period are shown in Figures 4.4 (a-c).
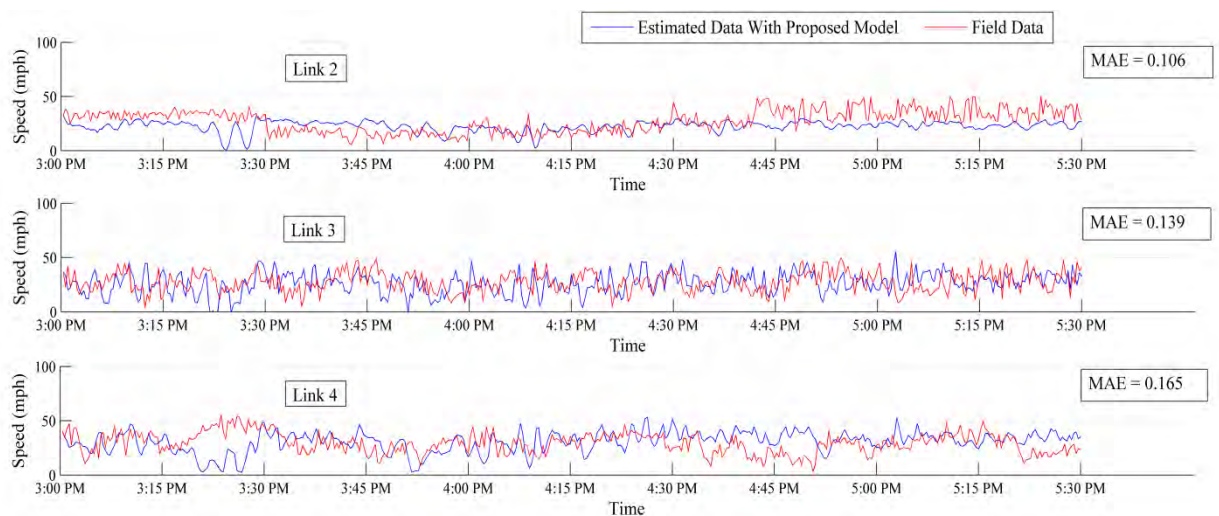
Figure 4.4 (a) Comparison between model estimated and field measured speed data for different links

45
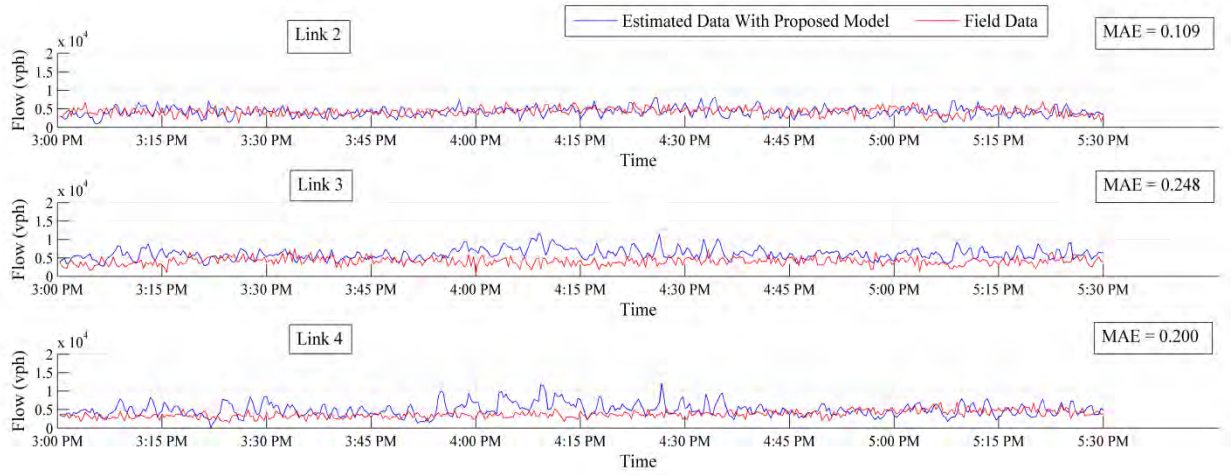
Figure 4.4 (b) Comparison between model estimated and field measured flow data for different links
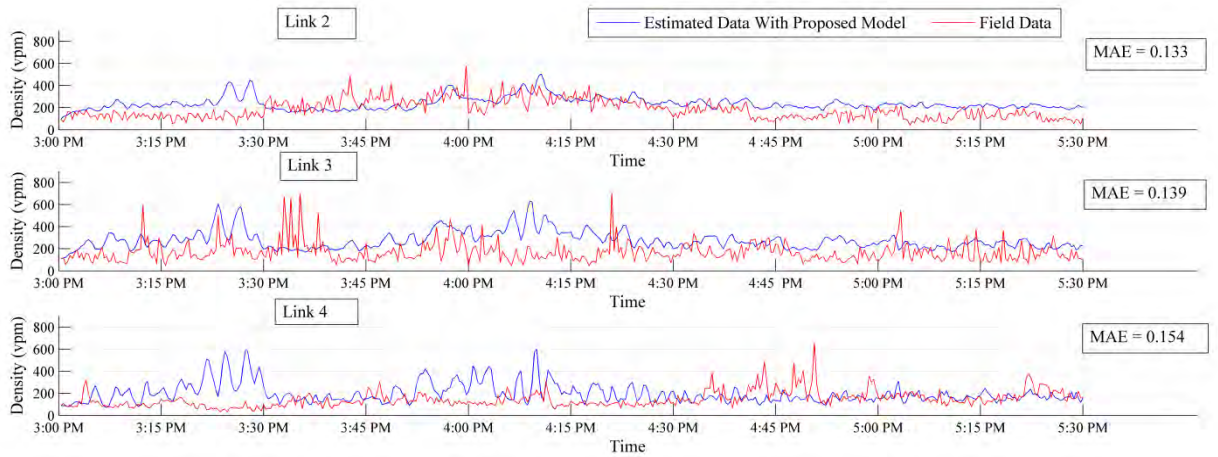
Figure 4.4 (c) Comparison between model estimated and field measured density data for different links

From qualitative analysis of these figures, it is seen that in general the proposed model can estimate the field traffic states quite accurately. However, the speed, flow and density of link 2 are estimated with greater accuracy than those of the other two links. Higher prediction error of links 3 and 4 may be attributed to their chaotic real-world traffic condition (which is also manifested in the form of reduced free flow speeds of these links) owing to greater roadside pedestrian activities.

As performance measure of the model, MAE is considered which quantifies the error between estimated and measured traffic states for the individual links. MAE is defined as:

$$\text{MAE}_i = \frac{\sum_{k=1}^{K=450} \left| \left(\text{Estimated} \, (v, \rho, q)_k - \text{Measured} \, (v, \rho, q)_k \right) \right|}{\sum_{k=1}^{K=450} \text{Measured} \, (v, \rho, q)_k}$$

TABLE 4.4 Sensitivity of the proposed model with respect to structural changes

Change in Model Structure	Link	MAE			f
		v	q	ρ	
Proposed Model	L2	0.106	0.109	0.133	1374 (n/a)
	L3	0.139	0.248	0.139	
	L4	0.165	0.200	0.154	
Fixed FD considering parameters of Link 2	L2	0.213	0.109	0.164	1846 (-34.3%)
	L3	0.333	0.251	0.149	
	L4	0.314	0.219	*0.129*	
Fixed FD considering parameters of Link 3	L2	0.107	*0.107*	0.150	1723 (-25.4%)
	L3	*0.099*	0.248	0.202	
	L4	0.179	0.290	0.242	
Fixed FD considering parameters of Link 4	L2	*0.101*	*0.107*	0.135	1578 (-14.8%)
	L3	*0.104*	0.248	0.146	
	L4	0.172	0.262	0.195	
Without θ	L2	0.212	*0.108*	0.164	1537 (-11.9%)
	L3	*0.109*	0.249	0.140	
	L4	*0.160*	0.239	*0.148*	
Without FD	L2	0.142	0.162	0.225	2386 (-73.6%)
	L3	*0.134*	0.300	0.284	
	L4	0.211	0.360	0.330	

(Note 1: In the table, the numbers in the first bracket denote the percentage change in overall model performance compared to the proposed model. Negative sign indicates that the overall performance of the model degrades due to the specific structural change.)
(Note 2: The italic number refers to a model structure that performs better compared to the proposed model structure in simulating the specific traffic parameter for the specific link. However, in those cases, the MAE values for proposed model and the specific case are found to be almost same.)

From Table 4.4, it is seen that the proposed model can simulate measured traffic states with an accuracy of 83.5-89.4% for speed estimation, 75.8-89.1% for flow estimation and 84.6-86.7% for density estimation. Such accuracy can be considered quite satisfactory given the wide variations in operating and performance characteristics of heterogeneous traffic. To investigate the improvement in traffic flow simulation accuracy achieved through each of the individual factors considered in developing the final model, different changed structures of the model are validated against real traffic data. These changes include: (1) dropping the stochastic flow and speed influencing terms (ξ_i^q and ξ_i^v); (2) using identical FD parameters for all the links instead of variable; (3) dropping the CF parameter θ; and (4) dropping the FD from the speed dynamics altogether. The function value f for each case is used for overall comparison of model performance. As expected, ξ_i^q and ξ_i^v play a very important role in the model, which fails to converge in their absence. After that, the use of variable FD for different links contributes a higher accuracy in simulating the flow by the model. The performance of the model degrades by 34.3%, 25.4% and 14.8% if fixed FD is considered with the parameters of links L2, L3

and L4 respectively. Dropping the CF parameter θ from the model results in an 11.9% increase in function value as compared to the full model. Interestingly, the simulation results show that the model performance degrades the most without the FD in the speed dynamics. Without FD, the error for traffic state estimation increases by 73.6% compared to the proposed model. Hence, in relation to the findings of Lu et al. (2011) (which concluded that model matching with FD and without FD does not make a significant difference on average for homogeneous traffic), it is seen that FD plays the most important role in the model for heterogeneous operating condition.

4.6 Conclusion

The current chapter focused on the development of a METANET-based stochastic model for simulating the heterogeneous traffic condition of Dhaka city. For this, at first the nature of the fundamental traffic relationships was systematically investigated based on the traffic data collected earlier. From regression analysis it was concluded that 3rd degree polynomial structure shows the best fit with the measured traffic data. Moreover, careful observation of the operating and performance characteristics of heterogeneous traffic revealed that classical traffic flow models tend to underestimate flow and speed due to the effect of vehicular influence area in the stated traffic condition. The model proposed in this research was developed taking these findings into account. Next, based on the field data, all relevant model parameters were estimated in model calibration, using an optimization technique. Then the calibrated model was used to successfully simulate traffic operations on the studied freeway in the model validation stage. Finally, investigation of different structural variations of the final model revealed that the stochastic state influencing terms and the FD (more specifically, link-specific FD) play the most important role in accurately estimating the traffic states in heterogeneous operating condition.

Chapter 5

Compatibility analysis of macroscopic and microscopic traffic simulation modeling

The evolution of advanced technologies and their application to modern traffic management systems require, in most cases, a combination of microscopic and macroscopic simulations. This necessitates the compatibility check between these two modeling approaches. The present chapter aims at comparing the performances of a microscopic simulation model, VISSIM (PTV 2010), and the macroscopic traffic flow model developed in the previous chapter, to evaluate how the change in traffic demand impacts the macroscopic simulation performance. For this, at first the need for such compatibility analysis is pointed out followed by earlier endeavours undertaken in this respect and the methodology adopted in the current research. Then details of the development, calibration and validation processes of the micro simulation model used in this study are provided. An experimental design is discussed, according to which data is compared and analyzed. Conclusions are presented after detailed discussions on the results of the analysis.

5.1 Significance of compatibility analysis

Due to model mechanisms, microscopic simulation models are often used in evaluating detailed local operations, such as congested intersections (Messer 1998), freeway bottlenecks (Halkias et al. 2007), weaving sections (Stewart et al. 1996), merging and lane changing (Hidas 2002), transportation corridor operations (Gomes et al. 2004), etc. They can also be used to analyze control scenarios, such as ramp control (Hasan et al. 2002, Beegala et al. 2005) and intelligent transportation strategies (Chu et al. 2004). However, this type of application is mainly off-line and lacks the predictive control functions. Instead, microscopic simulation is an effective tool to evaluate the performance of control measures before their implementation.

On the other hand, the application of macroscopic simulation models is aimed at large-scale roadway networks (Kotsialos et al. 2002, Carlson et al. 2010) or online (real-time) traffic control to reduce congestion and improve mobility (Lu et al. 2010, Hegyi et al. 2005a, Hegyi et al. 2005b). In Hegyi et al.'s (2005b) study, the authors used a macroscopic traffic flow model, METANET, as the state prediction model for optimal coordination of variable speed limits and ramp metering in a freeway network and found that the coordinated control can result in a higher outflow and a significantly lower total travel time in the road network.

Thus, the microscopic and macroscopic model outputs are used in different stages of the same model predictive control strategy. This calls for the compatibility analysis between these two modeling approaches, i.e. it is required to check whether both macroscopic and microscopic models provide similar traffic state results under all traffic conditions,

including light traffic, moderate traffic, heavy traffic and excessively congested traffic. If it does, the macroscopic model can be successfully used for on-line traffic state prediction under different demand scenarios.

An added advantage of a compatible macroscopic model is that the measured speed-flow relationship can be used directly as input parameters of the model, while the system parameters of the microscopic model (for e.g. VISSIM) do not directly correspond to the measured speed and flow values. Therefore, it is very difficult to calibrate the microscopic model for every geometric and traffic conditions. Moreover, being computationally less demanding, the macroscopic models consume much less computation time than the microscopic models, so that they are more suitable for short-time predictions. For all these reasons, compatibility analysis of macroscopic and microscopic traffic simulation modeling is gaining more importance day by day.

5.2 Previous studies on compatibility analysis of micro and macro traffic models

There are only limited studies on the comparison of macroscopic and microscopic model performances. Cluitmans et al. (2006) compared a macroscopic and a microscopic simulation model on a freeway in The Netherlands and concluded that both models used in their study were not able to simulate well when traffic demand was very high. Lamon (2008) used METANET and PARAMICS simulation on a freeway network of the Dutch city of Eindhoven for a short peak period. Both good agreement and wide discrepancies were observed between the outputs from the two models. Wu (2002) applied a macroscopic model NETCELL and VISSIM simulation for a congested freeway and found that NETCELL can reproduce the congested traffic condition much better than VISSIM, whereas the later can represent the real world traffic conditions better in free-flow. Ishak et al. (2006) evaluated the performance of the macroscopic model, CTM and the microscopic simulation model, CORSIM, on a congested freeway and showed that comparable performances of both simulation models (in terms of link density and total network travel time) can be obtained. Recently, Yin (2014) compared the performance of METANET with VISSIM simulation under different traffic levels and simulation time steps. Based on the performance of the two models it was concluded that consistent traffic states are obtained when traffic demand is at moderate to heavy level. However, under excessive traffic demand (stop-and-go conditions), significant differences exist between the simulated speed and density from the two models evaluated.

Literature review showed mixed results as to whether microscopic and macroscopic simulations have similar performances. As such, the current chapter focuses on the compatibility analysis of the METANET-based model for heterogeneous traffic developed in the previous chapter with the microscopic simulation model VISSIM. For application of the developed model for ATM purposes, systematic comparative study under varied traffic demand is required to calibrate and adjust the proposed macroscopic model for accurate traffic state estimation and prediction.

5.3 Methodology

In this portion of the study, the compatibility between the developed macroscopic model for heterogeneous traffic and the microscopic simulation model, VISSIM is analyzed on the test section of Figure 3.1. For this, the microscopic model, VISSIM, is calibrated and validated using field measured traffic volume and speed data. The METANET-based stochastic macroscopic simulation model is also calibrated and validated for the same section of urban arterial and for the same field data. This study considers the effect of various traffic demands on the compatibility of the macroscopic and microscopic simulation models. The macroscopic simulation model was run with four different levels of traffic demands and compared with the outputs from the microscopic simulation with the same initial traffic states. The prediction errors from the macroscopic model are used as measures of effectiveness (MOE) and are evaluated with respect to traffic demand. The conclusions are obtained from the comparative analysis. Figure 5.1 is the flowchart showing the methodology of this compatibility study.
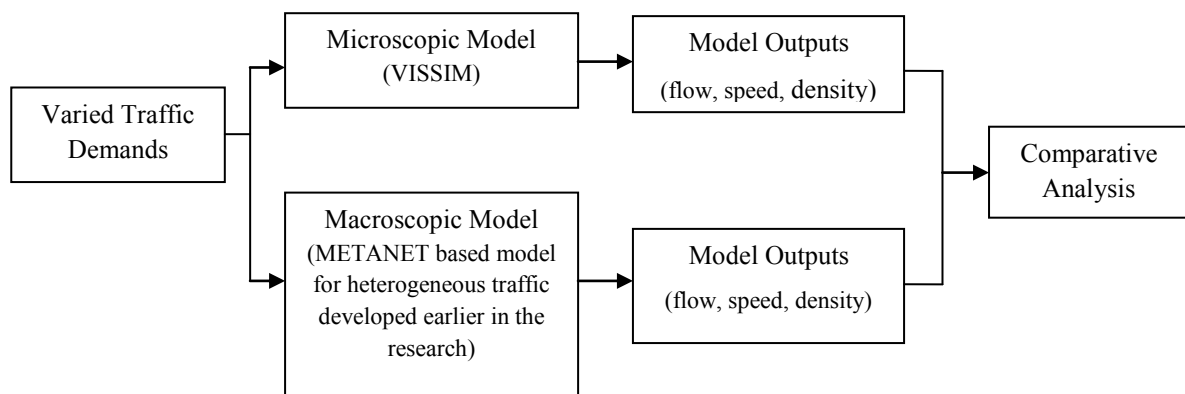
Figure 5.1 Flow chart showing methodology of compatibility analysis

5.4 Microscopic simulation model

In this study, a very popular microscopic simulation package, VISSIM, was used. VISSIM is a time step and behavior-based simulation model developed to represent urban traffic and public transport operations and flows of pedestrians. The following sub-sections present the details of the development of a candidate microscopic model of the test site.

5.4.1 Building base model of the test site

At first, detailed network geometry data (following a detailed corridor survey conducted by the researcher and the roadway map obtained by the courtesy of Google maps), including the exact location of on-ramps and off-ramps was coded through the VISSIM graphical user interface (GUI). This microscopic simulation package uses a link-and-connector approach to represent roadway sections and merge/diverge points. Links were used to build the test section. A number of attributes were assigned to the links, including number of lanes, lane widths, road gradient, as well as car-following and lane-changing behaviours. Connectors were used to connect the links to build the entire test section. All of the turning movements at roadway merging/diverging points were joined by

connectors. After the network coding, the base model was run with certain mainline and on-ramp demand and default driver behavior parameters; and traffic operation was observed at on-ramps, merge sections and diverge sections. Second, this research adjusted several operational parameters (as follows), so that the model replicates real-world traffic operations of the test site. During simulation, virtual loop detectors were placed on each lane of each segment as well as at the on- and off-ramps (at approximately the same location as the video cameras) to measure flow and speed.

5.4.2 Base model calibration

Calibration is the process by which individual components of a simulation model are refined and adjusted, so that the model accurately represents field measured or observed traffic conditions. In micro simulation model calibration is conducted from the following two points of view.

5.4.2.1 System calibration

In the VISSIM model, vehicles were loaded into the roadway according to a predefined distribution based on total traffic demand. The traffic data for the mainline as well as for the on and off-ramps was extracted from video footages of 15th April, 2015. Six vehicle types were created to replicate traffic composition in the test site: (1) Car (40.0%); (2) Microbus/jeep (12.0%); (3) Motorcycle (10.0%); (4) Bus (8.0%); (5) Utility/Leguna (10.0%); and (6) Auto-rickshaws/CNG (20.0%). Local vehicles like CNG and Leguna were modeled in 3D Studio-Max first and then converted into recognizable vehicle element of the micro simulator (Figure 5.2). The simulation warm-up period was set to 15 minutes.

Figure 5.2 Customized 3-D models of CNG and Leguna

Vehicles were calibrated for the desired speed distribution, acceleration, deceleration as well as for the physical dimensions. Here it can be mentioned that VISSIM does not use a single acceleration and deceleration value but uses functions to represent the differences in a driver's behavior. For each vehicle type two acceleration functions (maximum and desired) and two deceleration functions (graphs) need to be assigned. The calibrated

values of these functions are given in Table 5.1 below. As an example, the acceleration and deceleration graphs for car as used in the base model are shown in Figure 5.3.

Table 5.1 Distribution of kinematic parameters of different vehicle types

Vehicle Type	Desired Speed (km/h)	Acceleration (m/s²)		Deceleration (m/s²)	
		Max.	Desired	Max.	Desired
Car	60	3.5	3.5	7.5	2.8
Microbus/Jeep	45	6.8	4.0	5.5	1.3
Motorcycle	40	3.5	3.5	7.5	2.8
Bus	45	1.2	1.2	7.5	0.9
Utility/Leguna	40	3.5	2.3	6.5	2.5
Auto-rickshaw/CNG	40	3.3	2.0	7.6	2.5
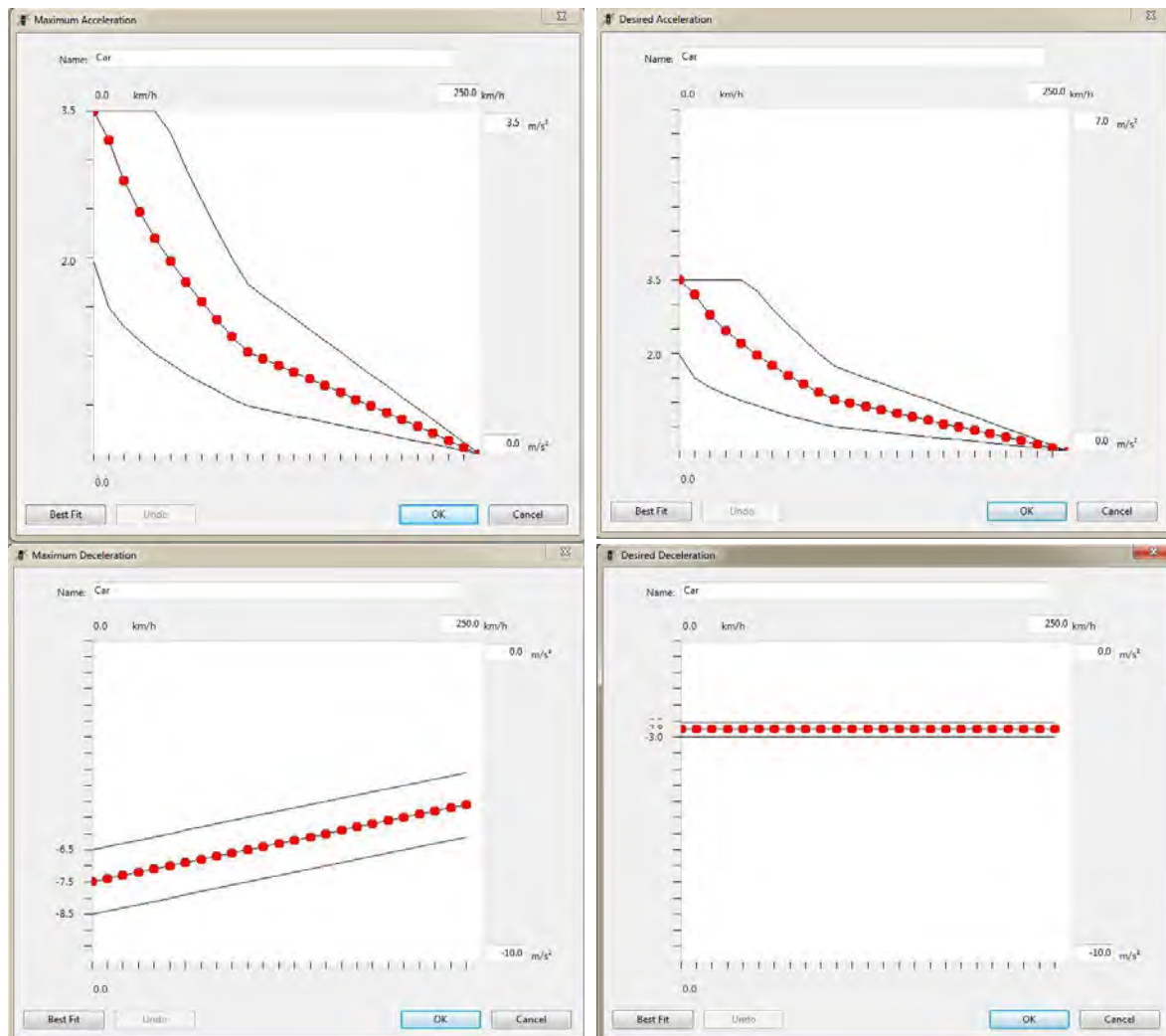
Figure 5.3 Maximum and desired acceleration and deceleration functions for car

5.4.2.2 Operational calibration

To precisely replicate the actual traffic behaviour of the test corridor, five customized link behavior types were defined: one for each of the five discretized segments (links). In addition, two other link behaviours were defined for the merge and diverge sections respectively. In VISSIM, the driving behaviour parameter sets for the customized freeway links were adjusted to alter the aggressiveness of the drivers to match the field condition. The calibrated parameters related to lane-changing and lateral movement of vehicles are shown in Table 5.2.

Table 5.2 Calibrated driving behaviour parameters

Parameters		Calibrated Values	Default Values
Car Following			
Observed Vehicles		8	2
Standstill Distance (m)	Link 2	0.7	1.5
	Link 3	0.7	1.5
	Link 4	0.7	1.5
Headway Time (s)	Link 2	2.5	0.9
	Link 3	2.5	0.9
	Link 4	2.7	0.9
Lane Changing			
Waiting Time before Diffusion (sec)		40	60
Overtake Reduced Speed Area		Allowed	Not Allowed
Lateral			
Desired Position at free flow		Any	Middle of lane
Observe vehicles on next lane(s)		Allowed	Not Allowed
Diamond shaped queuing		Allowed	Not Allowed
Consider next turning direction		Allowed	Not Allowed
Minimum Lateral Distance (m)	Distance at 0 km/h	0.4	1.0
	Distance at 50 km/h	0.5	1.0
Overtake on Same Lane	On Left	Allowed	Not Allowed
	On Right	Allowed	Not Allowed

Specifically, the standstill distance CC0 was changed from the default value of 1.5 m to 0.7 m for all the intermediate links to replicate the tendency of the drivers of the study site to keep minimum possible distance between stopped vehicles. Moreover, the headway time (CC1) was set to 2.50, 2.50, and 2.70 for links L2, L3 and L4 respectively, from the default value of 0.9 seconds. These parameters were adjusted with trial-and-error method and numerous iterations, until the simulated flow and speed were within 10% of the field traffic data. Note that, CC1, which controls the safety distance in the car-following logic

of VISSIM (Wiedemann, 1999), has the strongest influence on freeway capacity adjustment. As a guideline, when all other operational parameters in VISSIM are kept in their default values, increasing CC1 results in consistent reduction of freeway capacity. Using this knowledge, the default value of CC1 was increased for each of the test links to simulate their reduced capacities under non-lane-based heterogeneous operation. Default values of the remaining eight parameters of Wiedemann's 1999 car following model were not altered, since their effect on overall model performance improvement is rather limited. Figure 5.4 shows the calibrated base model of the study corridor in VISSIM interphase.


Figure 5.4 Calibrated base model of the test site with background map

5.4.3 Base model validation

The calibrated base model was further validated against field data of 16th April, 2015. This research adopts the Geoffrey E. Heavers (GEH) statistic to compare field measured volumes with those obtained from the VISSIM base model. GEH value is defined as:

$$GEH = \sqrt{\frac{(simulated - observed)^2}{0.5(simulated + observed)}}$$

As a general guideline for model validation, GEH values less than 5 indicate good fit; values between 5-10 require further investigation, while values above 10 indicate a poor fit (Holm et al. 2007). However, this guideline is for homogeneous traffic following strict lane discipline. For non-lane-based heterogeneous mix, owing to the wide variation in the operating and performance characteristics of vehicles, the thresholds of the GEH values are likely to be more lenient. From this consideration, GEH values below 10 can be taken to indicate good fit for heterogeneous traffic. This research obtained average GEH values of 7.50, 7.37 and 9.02 for links L2, L3 and L4 respectively (Figure 5.5 (a-c)). Thus the microscopic model of the test site is well calibrated and validated and can represent the field traffic condition with remarkable accuracy.
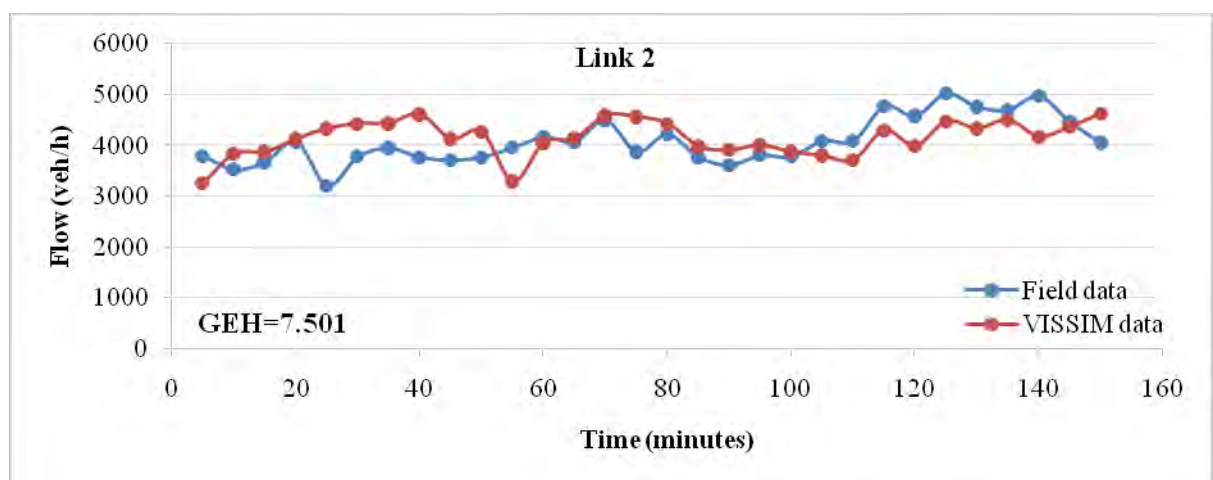
(a)
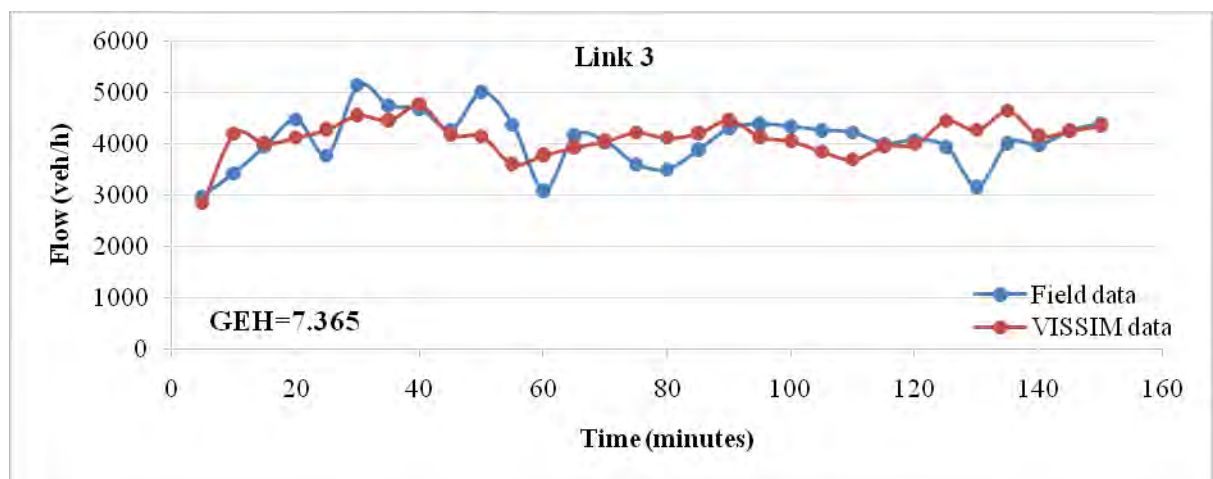
(b)
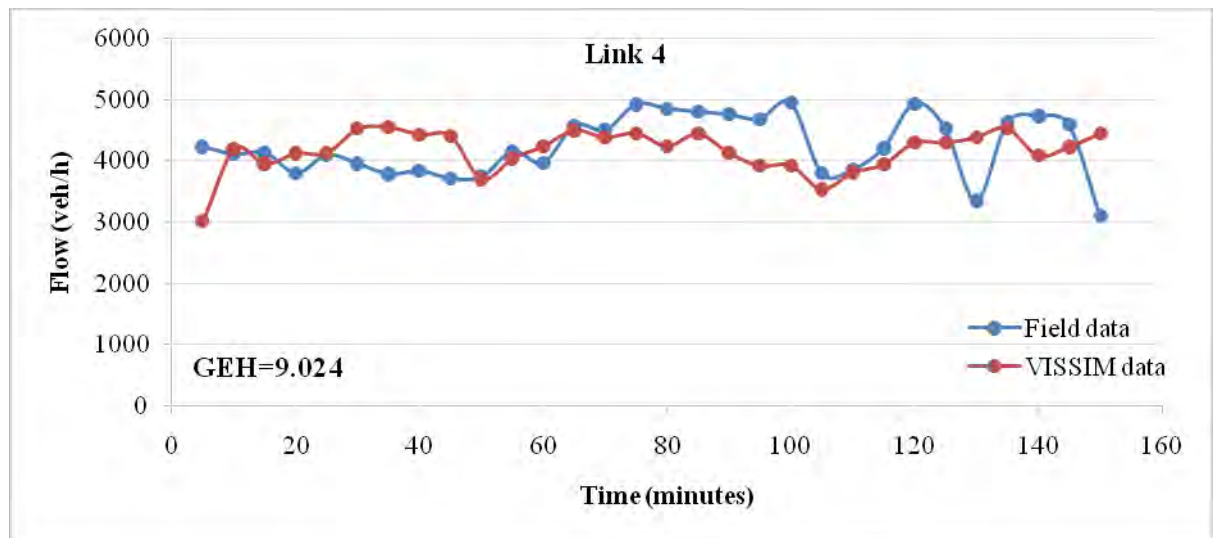
(c)

Figure 5.5 Comparison between field and micro simulation data for VISSIM model validation (5 minutes resolution field data used in the plots was collected from 3:00 PM to 5:30 PM on 16th April, 2015.)

5.5 Macroscopic simulation model

The macroscopic simulation model used for the compatibility analysis is the stochastic second-order model developed for heterogeneous traffic in the previous chapter. The proposed macro model was calibrated and validated using the same data sets as the microscopic model. So here details of these processes are not provided again. The VISSIM outputs (flow and speed) were aggregated for 20 seconds and used as initial inputs for the macroscopic simulation model.

5.6 Experimental design

To evaluate the compatibility of microscopic and macroscopic simulation models, a range of traffic demand should be tested to compare model performance under varied traffic conditions. The traffic demands should cover the practical range of operations in typical traffic flow control applications. In very light traffic demands, traffic management and control measures are not required. In this study, four traffic demand levels were used to run the microscopic and macroscopic simulations. Considering the measured traffic flow of 16th April, 2015 as moderate demand, it was artificially increased in two steps of 10% and then reduced by 20% to generate the four different levels of traffic demands: light demand (approximately 850 veh/h/lane at the mainline origin), moderate demand (1000 veh/h/lane), heavy demand (1200 veh/h/lane) and excessive demand (1300 veh/h/lane). Here, the traffic demand was increased step by step because it is more crucial to accurately identify the nature of model performance in over-saturated condition as compared to relatively non-congested condition of the roadway. However, for the various traffic demand levels, demand at on-ramps and the proportion of vehicles that exit from off-ramps were kept the same as in the field traffic demand level, since the centre of attention here is the compatibility check of model performance for the main line.

57

5.7 Data analysis and discussion

For each traffic demand level, VISSIM was run for 2 hours and 45 minutes. Excluding the warm-up time of 15 minutes, a maximum of 2 hours and 30 minutes of usable data was obtained for the study. The output from VISSIM was aggregated to data sets having 20 seconds time step length to run the developed macroscopic model.

For the data analysis, the outputs from VISSIM were taken as the ground truth and the outputs from the macroscopic model were compared with those from the VISSIM model. Based on this comparison, the effect of different levels of traffic demand on the developed macroscopic model is evaluated. The following figures (Figures 5.6-5.8) show the qualitative differences between the individual link traffic states coming from VISSIM, and the corresponding data coming from the calibrated macro model for the four different levels of traffic demand considered.
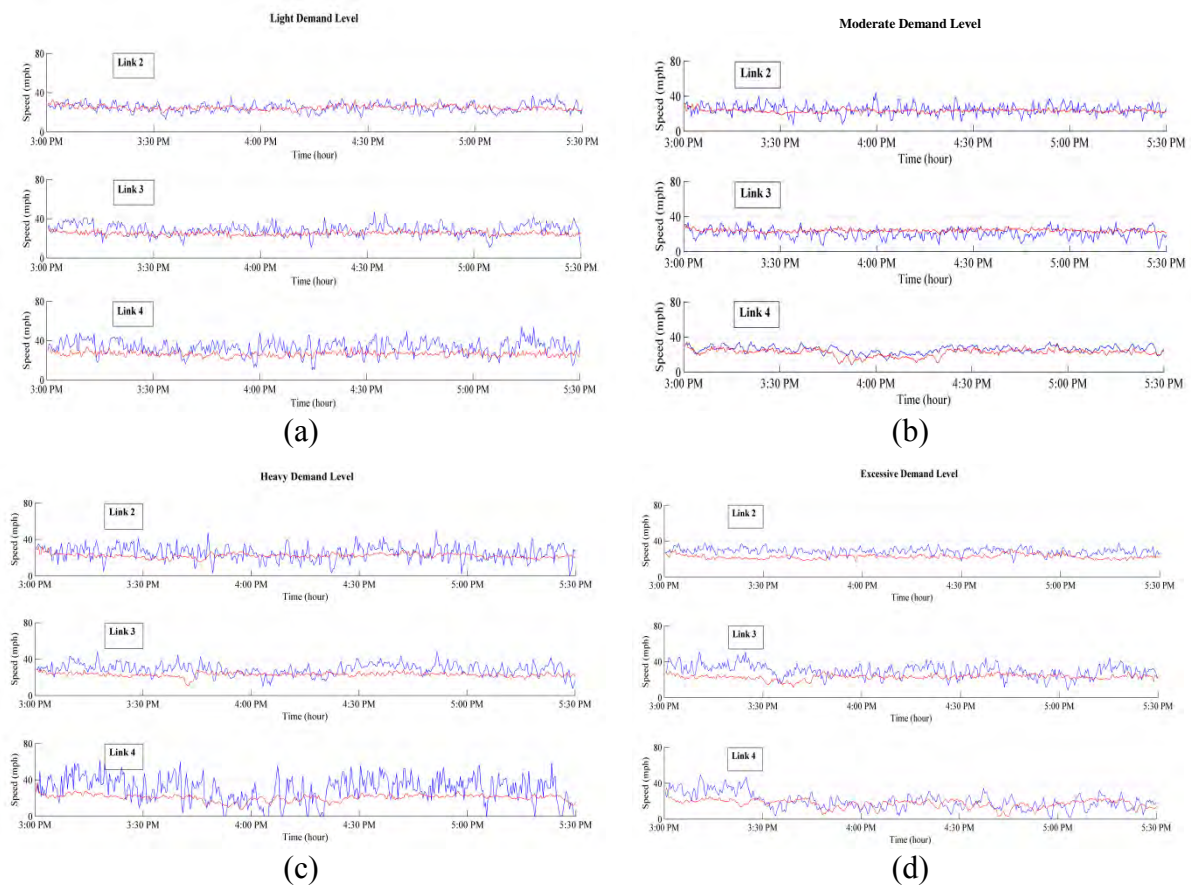
Figure 5.6 (a-d) Comparison between VISSIM (━━) and macro models' (━━) speed outputs at four different traffic demand levels
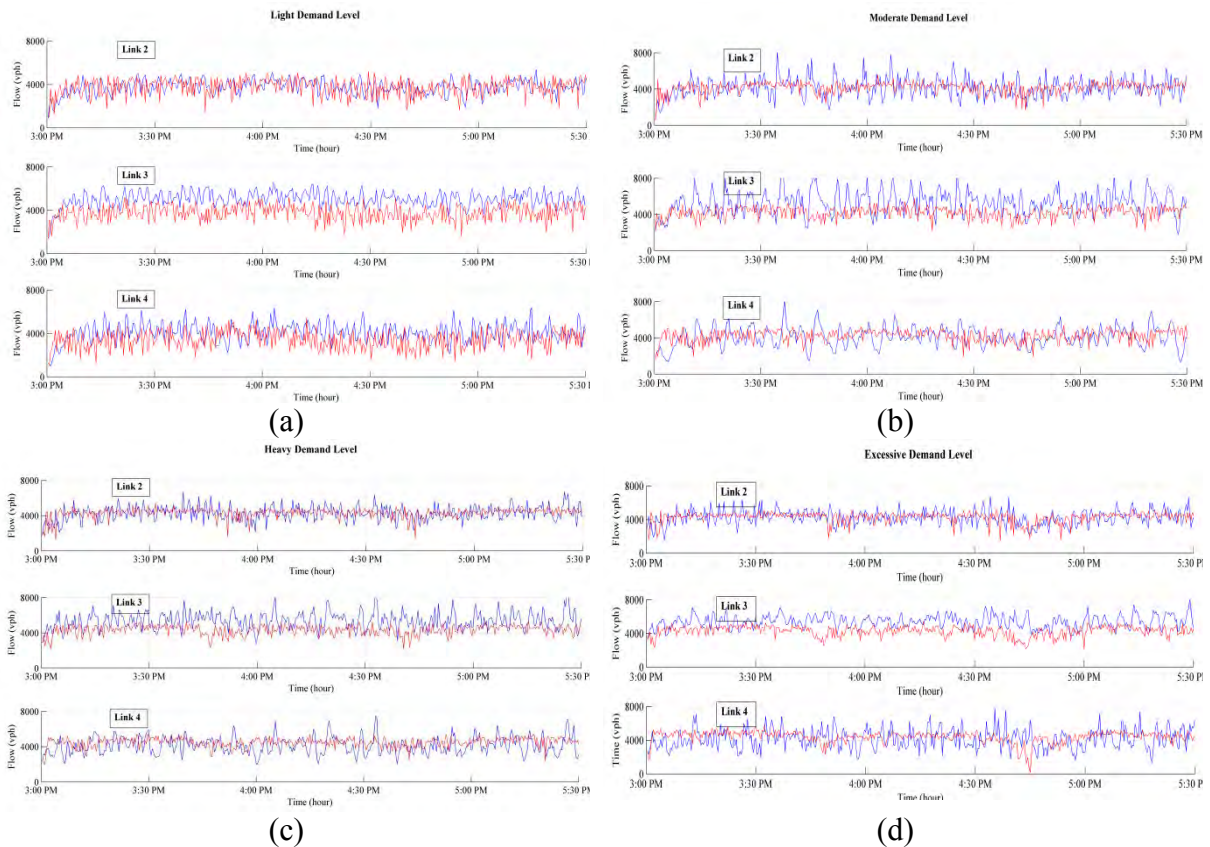
Figure 5.7 (a-d) Comparison between VISSIM (——) and macro models' (——) flow outputs at four different traffic demand levels
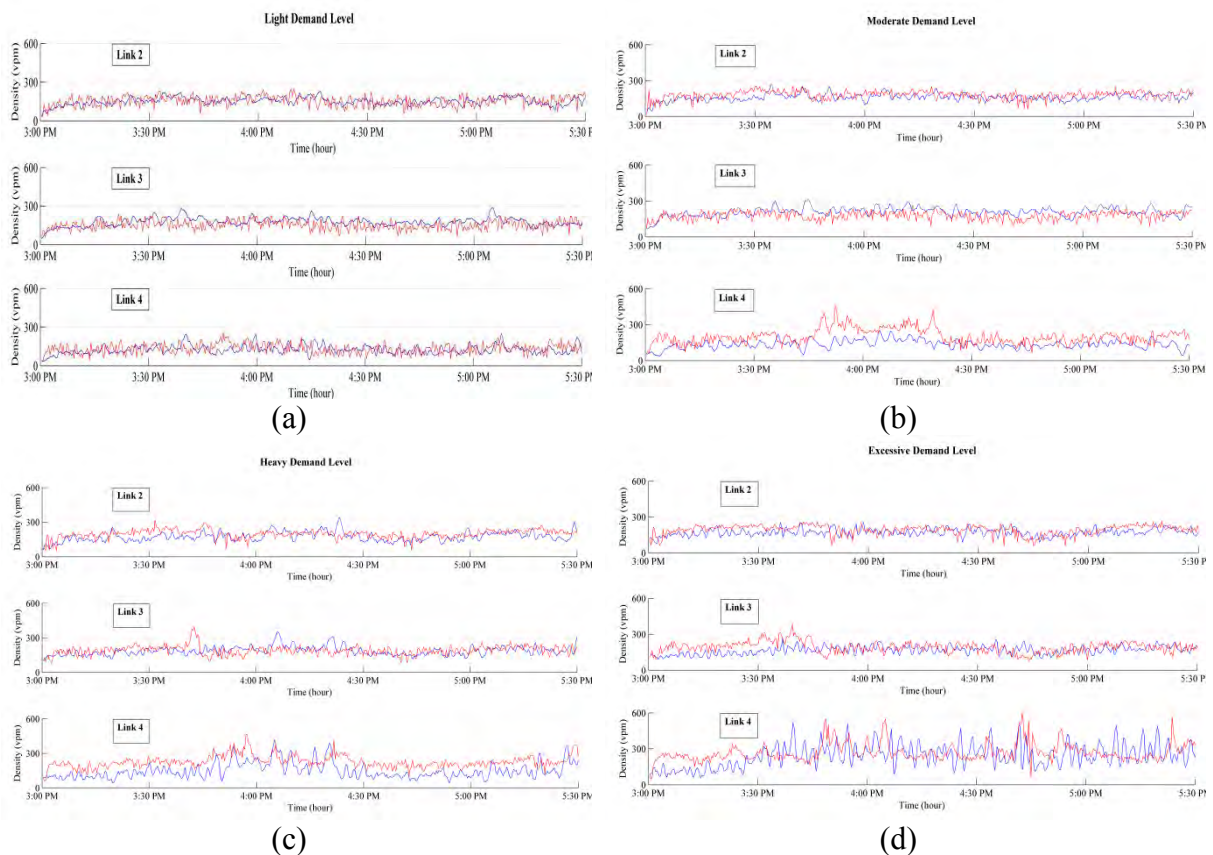
Figure 5.8 (a-d) Comparison between VISSIM (——) and macro models' (——) density outputs at four different traffic demand levels

From qualitative analysis, it is seen that the outputs from the macroscopic and the VISSIM models have the same trends over the whole range of traffic demand levels tested. The outputs from the models are also spatially consistent with each other. Thus, in general, the developed macroscopic model is compatible with the VISSIM model.

Closer look at the figures reveals that the macroscopic model tends to slightly over-estimate the flow of link 3 for the light and moderate traffic demand levels (Figures 5.7a and 5.7b). This may be partially attributed to the inflow from on-ramp, and partially to the combined stochastic natures of the macroscopic and microscopic simulations

For quantitative analysis, the MAE between the macroscopic and microscopic model outputs for the individual links is used as the measure of performance of the developed macro model. The link-wise MAEs of speed, flow and density estimation under varying traffic demand are given in Table 5.3.

Table 5.3 Comparison of prediction accuracy of the macroscopic model under varying traffic demands

Traffic Demand Levels	Link	MAE		
		v	q	ρ
Light	L2	0.04989	0.06575	0.07958
	L3	0.07362	0.11853	0.08816
	L4	0.10981	0.09244	0.09358
Moderate	L2	0.07192	0.06998	0.06427
	L3	0.07288	0.11176	0.07860
	L4	0.06315	0.07764	0.12929
Heavy	L2	0.10655	0.05302	0.06835
	L3	0.11049	0.09238	0.06677
	L4	0.20140	0.06916	0.14254
Excessive	L2	0.10444	0.05836	0.06342
	L3	0.13496	0.09241	0.07634
	L4	0.11792	0.08731	0.13981

The traffic demand effects on simulation performance are shown in Figures 5.9, 5.10 and 5.11 as well. It is seen that, over the whole range of traffic demand, the macroscopic model estimates the outflow of the test section with greater accuracy than speed or density. Also the MAE in traffic state estimation of the links does not increase or decrease in cumulative rate with the change in demand levels. Thus, no distinct trend is found in the MAEs of all the three traffic states estimated i.e. speed, flow and density. This is good from modeling point of view, since it indicates that the model performs quite satisfactorily over the whole range of traffic demand levels.
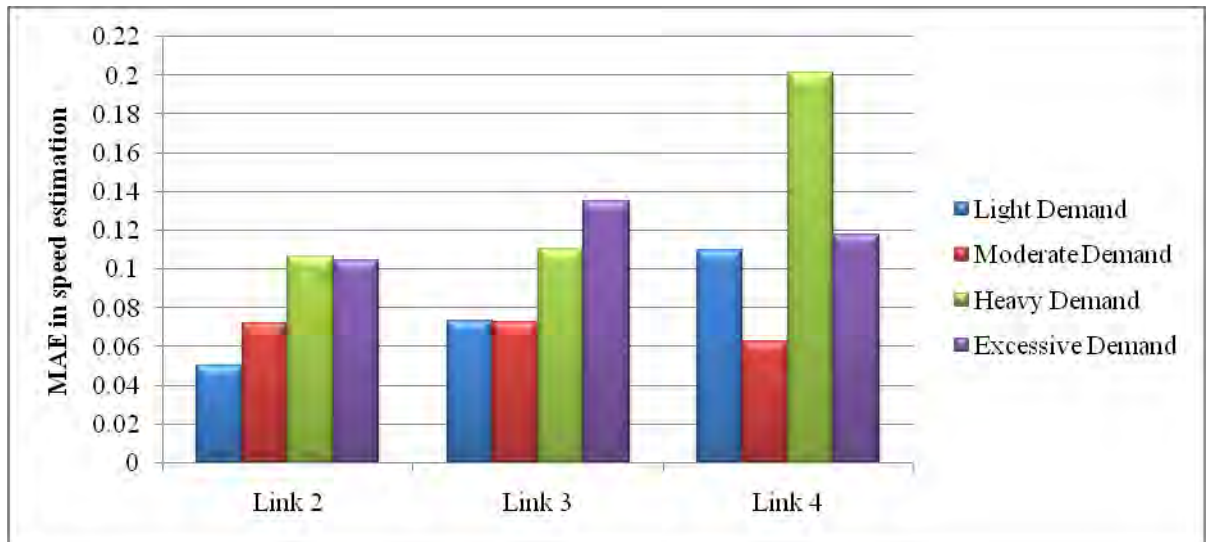
Figure 5.9 Link-wise MAEs in simulating speed by the developed macroscopic model for different demand levels
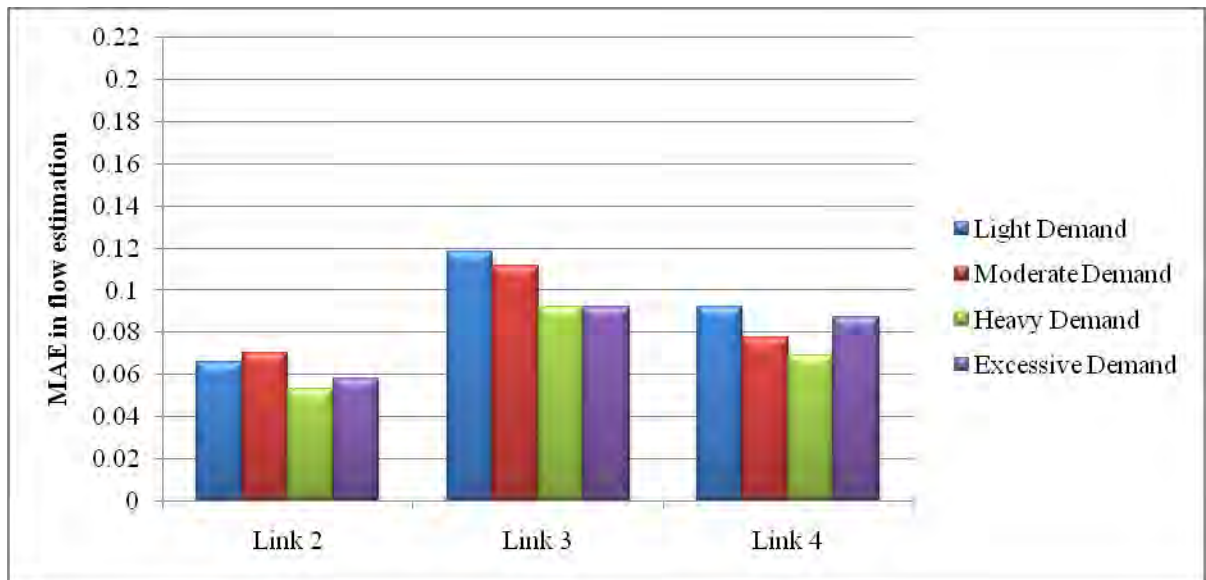
Figure 5.10 Link-wise MAEs in simulating flow by the developed macroscopic model for different demand levels
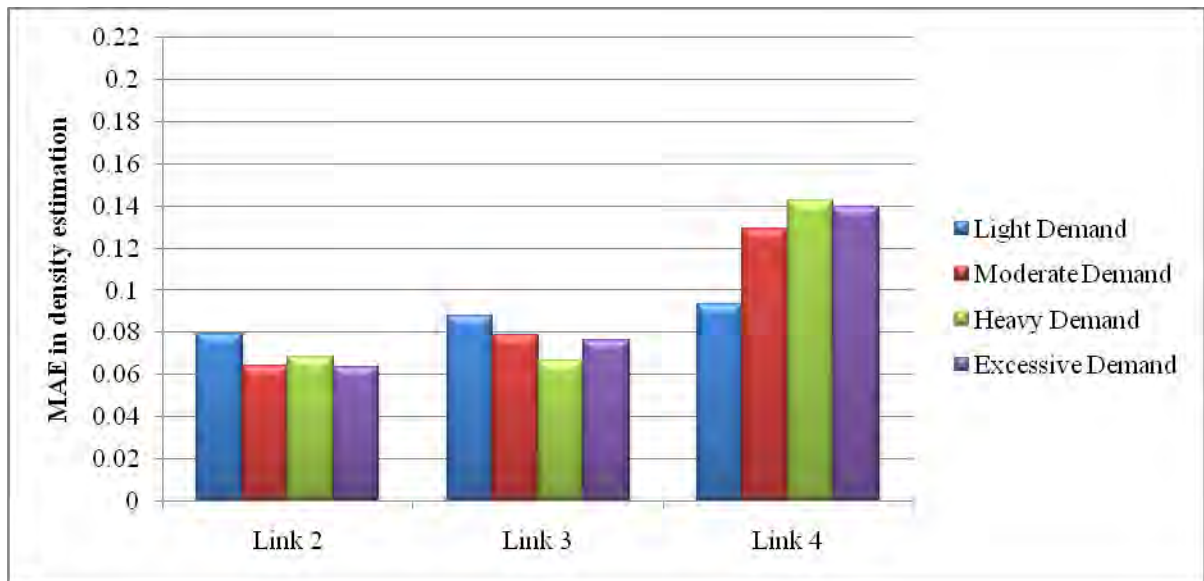
Figure 5.11 Link-wise MAEs in simulating density by the developed macroscopic model for different demand levels

While comparing the VISSIM and macroscopic models' speed and density outputs in different links, it was found that link 4 tends to generate greater prediction error than the other links over the whole range of traffic demand levels. This may be attributed to the chaotic real-world traffic condition of this link owing to greater roadside pedestrian activities.

5.8 Conclusion

This chapter compared the performance of the proposed macroscopic simulation model with a microscopic simulation model, VISSIM, under different traffic levels. Based on the performance of the two models and the comparison analysis presented above, it was concluded that the prediction of traffic states from the macroscopic model is generally consistent with that from VISSIM simulation. Also, the MAEs in traffic state estimation of various links do not show any distinct trend with the change of traffic demand levels, thus indicating that the developed macroscopic model performs quite satisfactorily over the whole range of traffic demand levels used in this research.

Chapter 6

SUMMARY AND CONCLUSIONS

6.1 Conclusions

This research developed a stochastic METANET-based model for heterogeneous traffic operations. For this, it investigated several important issues in traffic flow modeling and simulation of freeways with heterogeneous traffic composition. These include the nature of the fundamental relationships among speed, flow and density for the stated operating condition, the compatibility of microscopic and proposed macroscopic traffic simulation on freeways, the effect of different levels of traffic demand on the simulation performance of the proposed model etc. Main conclusions from this research are summarized chapter-wise below.

Chapter 2 provided an overview on the state-of-the-art of traffic flow models with a special focus on microscopic car-following models and second-order macroscopic models. The traffic models were reviewed with respect to their categories in terms of level of detail, scale of independent variables, nature of independent variables and model representations. Various microscopic car-following model formulations, ideologies and properties were discussed. On the macroscopic level, both first and second-order models and their respective advantages and disadvantages were presented. The comprehensive review of the vast literature on macroscopic traffic flow modeling revealed very limited studies on the understanding of traffic flow for non-lane-based heterogeneous traffic in developing countries. Difficulty of high-resolution data collection and the complex nature of the traffic dynamics have been pointed out as the main reasons behind such limited research in this sector. As such, this study mainly focused on introducing a practical method of high-resolution data collection and proposing a macroscopic flow model having both speed and density dynamics for the stated traffic condition.

Chapter 3 mainly focused on the data collection and processing techniques adopted in this research. It presented the geometric and traffic characteristics of the study site along with the details of the discretization process and the high-resolution traffic data collection method. It then briefly discussed the image processing technique used here for extracting flow and speed data from the video footages of the test site. The measured high-resolution data was used for the development and analysis of the macro and micro models in the subsequent chapters. Some justifications regarding the choice of methods employed were also provided.

Chapter 4 is the most important part of this study. Here, an in-depth investigation was done for understanding the macroscopic speed-flow-density relationships in the heterogeneous-flow condition of the test site. The main findings of this investigation are listed below:

(1) Differences in microscopic non-lane-based heterogeneous traffic characteristics

result in different macroscopic behaviour of the traffic stream in comparison to the lane-based homogeneous operating condition.

(2) According to the regression analysis of the field data, the FD (speed-density) has a 3rd degree polynomial structure for all the links investigated, which differs from the findings of Chari & Badarinath (1983). However, comparison of the R-Square values obtained in the previous studies reveals better fitness of the polynomial structure for the current traffic condition.

(3) Although the structure of the FD remains the same over the links, the parameters (v_j and ρ_j) obtained from the regression analysis of measured $v - \rho$ plots, appear to be affected by roadside friction. In particular, increment of pedestrian activities on raised sidewalk along the study section increases the associated link jam density and reduces free-flow speed.

(4) State-of-art state estimation equations tend to underestimate the actual traffic states in non-lane-based heterogeneous condition due to the effect of vehicular influence area.

(5) Moreover, the anticipation behaviour of drivers in such traffic condition is dependent on the speed of multiple leaders instead of just the immediate downstream density.

Based on the above findings, this research proposed a new METANET-based traffic flow model having the following special features: (1) both the flow and speed dynamics have a normally distributed stochastic terms with particular mean and standard deviation parameters; (2) the FD in the speed dynamics follows Zhang's (1999) one-parameter polynomial structure to allow for generalization and data-fitting flexibility; and (3) the parameters of the FD are variable over the links.

In the model calibration stage, simultaneous optimization of FD parameters and driver-related parameters were conducted. Interestingly, the optimized values of v_j and ρ_j obtained here follow similar trend to the values obtained when FD was calibrated in stand-alone mode (Figure 4.2 (a-c)). Thus, the optimized parameters capture the existing traffic conditions of the respective links quite well. Finally, to determine the individual contributions of the proposed model features, different structural variations of the final model were investigated. It was estimated that the link-specific FD parameters and the stochastic traffic state influencing terms ξ_i^q and ξ_i^v improve the model performance the most, followed by the CF parameter θ. Another interesting finding is that the proposed model performs most poorly in the absence of FD in the speed dynamics, which is in contrast to the findings of Lu et al. (2011) for lane-based homogeneous traffic. Thus it can be concluded that FD affects the traffic states very seriously for heterogeneous composition and cannot be dropped off from the speed dynamics for simplicity in control design.

Chapter 5 systematically investigated the compatibility between microscopic and macroscopic simulation models. The focus of this analysis was to find out the effect of traffic demand on model performance. The predicted speed, flow and density from the developed macroscopic model were compared with those from a microscopic simulation model, VISSIM, on the test section of Figure 3.1. Four levels of traffic demands viz. light, moderate, heavy and excessive demand levels were applied to evaluate the compatibility of the two models. Based on the performance of the models and comparative analysis, the following main conclusions were found:

(1) The prediction of traffic states from the proposed stochastic METANET-based model is generally consistent with that from VISSIM simulation over the whole range of traffic demand levels used in this research.

(2) The MAEs in traffic state estimation of various links do not show any distinct trend with the change of traffic demand levels, thus indicating that the developed macroscopic model performs quite satisfactorily for different traffic demand levels.

6.2 Recommendations for future research

Although traffic flow models have been studied for more than half a century in the developed world, research on this topic in Bangladesh as well as in other south-east Asian countries is extremely scarce and challenging. This is mainly due to the complexity of data collection and processing and the wide variations of driver population, vehicle components and traffic environment. Even though the current study tried to focus some effort in this sector, it cannot be viewed as a complete understanding of the highly complex heterogeneous traffic operation. In fact, it should be kept in mind that there is not a single traffic model that applies to all traffic situations. Further research to explore other forms of the traffic flow models for better representation of the heterogeneous traffic state evolution and traffic control is desirable in both theoretical analysis and field applications. In this section some recommendations are provided for future research following the studies carried out in this dissertation. These are listed below.

- Several features of the proposed model could be the subject of more extensive research, including the nature of the stochastic state influencing terms which are assumed to be normally distributed in this study.

- Sensitivity investigations of the calibrated model parameters should be done for checking the transferability of the model for changed application conditions.

- Also, in the compatibility analysis of microscopic and macroscopic simulation models, the effect of various time-step lengths on macroscopic model performance should be evaluated. Thus the most appropriate time-step length could be determined that will be used for on-line traffic control purpose on the studied urban freeway.

- Moreover, the impact of merging and diverging sections (at ramp locations) on macroscopic model performance should be investigated to provide experimental evidence as to whether explicit merging or diverging terms should be included in the speed dynamics of the proposed stochastic METANET-based traffic simulation model.

- In future studies it is recommended that different objective functions be used for calibration of the model parameters to investigate if the result is robust. Also, other optimization algorithms can used to investigate how the optimal set of parameters depends on the choice of the algorithm.

- Finally, if field traffic states change dramatically over a very short time period, application of online calibration is recommended to adjust the model for such traffic conditions.

REFERENCES

Alexiadis, V., Gettman, & Hranac, R. (2004). Next Generation Simulation (NGSIM): identification and prioritization of core algorithm categories. *Department of Transportation Federal Highway Administration (FHWA).*

Algers, S., Bernauer, E., Boero, M., Breheret, L., Di Taranto, C., Dougherty, M., Fox, K., & Gabard, J. F. (1997) Review of Micro-Simulation Models. Review Report of the SMARTEST project; deliverable 3, 1997.

Arasan, V. T., & Koshy, R. Z. (2005). Methodology for modeling highly heterogeneous traffic flow. *Journal of Transportation Engineering*, *131*(7), 544-551.

Aw, A., & Rascle, M. (2000). Resurrection of" second order" models of traffic flow. *SIAM journal on applied mathematics*, *60*(3), 916-938.

Bando, M., Hasebe, K., Nakanishi, K., & Nakayama, A. (1998). Analysis of optimal velocity model with explicit delay. *Physical Review E*, *58*(5), 5429-5435.

Beegala, A., Hourdakis, J., & Michalopoulos, P. (2005). Methodology for performance optimization of ramp control strategies through microsimulation.*Transportation Research Record: Journal of the Transportation Research Board*, (1925), 87-98.

Bellemans, T. (2003). Traffic control on motorways. *PhD dissertation. Katholieke Universiteit Leuven, Belgium.*

Brackstone, M., & McDonald, M. (1999). Car-following: a historical review.*Transportation Research Part F: Traffic Psychology and Behaviour*, *2*(4), 181-196.

Cassidy, M. J., & Bertini, R. L. (1999). Observations at a freeway bottleneck.*Transportation and Traffic Theory*, 107-146.

Chandler, R. E., Herman, R., & Montroll, E. W. (1958). Traffic dynamics: studies in car following. *Operations research*, *6*(2), 165-184.

Chari, S. R., & Badarinath, K. M. (1983). Study of mixed traffic stream parameters through time lapse photography. In *Highway Research Bulletin, Indian Roads Congress* Vol. 20, pp. 57-83.

Chu, L., Liu, H., & Recker, W. (2004). Using microscopic simulation to evaluate potential intelligent transportation system strategies under nonrecurrent congestion. *Transportation Research Record: Journal of the Transportation Research Board*, (1886), 76-84.

Cluitmans, M., Griez, T., Jacobs, K., Krieger, T. and Mehlkop, B. (2006). Comparison of a microscopic and a macroscopic model for the simulation of traffic flow phenomena. Maastricht University, The Netherlands.

Cremer, M., & May, A. D. (1986). An extended traffic flow model for inner urban freeways. In *5th IFAC/IFIP/IFORS International Conference on Control in Transportation Systems, Vienna, Austria,* 383-388.

Cremer, M., & Papageorgiou, M. (1981). Parameter identification for a traffic flow model. *Automatica*, *17*(6), 837-843.

Daganzo, C. F. (1994). The cell transmission model: A dynamic representation of highway traffic consistent with the hydrodynamic theory. *Transportation Research Part B: Methodological*, *28*(4), 269-287.

Daganzo, C. F. (1995a). The cell transmission model, part II: network traffic. *Transportation Research Part B: Methodological*, *29*(2), 79-93.

Daganzo, C. F. (1995b). Requiem for second-order fluid approximations of traffic flow. *Transportation Research Part B: Methodological*, *29*(4), 277-286.

Daganzo, C. F., Lin, W. H., & Del Castillo, J. M. (1997). A simple physical principle for the simulation of freeways with special lanes and priority vehicles. *Transportation Research Part B: Methodological*, *31*(2), 103-125.

Edie, L. C. (1961). Car-following and steady-state theory for non-congested traffic. *Operations Research*, *9*(1), 66-76.

Eidehall, A., Pohl, J., Gustafsson, F., & Ekmark, J. (2007). Toward autonomous collision avoidance by steering. *IEEE Transactions on Intelligent Transportation Systems, 8*(1), 84-94.

Evans, L., & Rothery, R. (1977). Perceptual thresholds in car following – a recent comparison. *Transportation Science, 11*(1), 60-72.

Feldman, O., & Maher, M. (2002). Optimisation of traffic signals using a cell transmission model. In *34th Annual Universities' Transport Study Group Conference, Napier University, Edinburgh*.

Forbes, T. W., Zagorski, H. J., Holshouser, E. L., & Deterline, W. A. (1958). Measurement of driver reactions to tunnel conditions. In *Highway Research Board Proceedings*, 37, 345-357.

Fritzsche, H. T. (1994). A model for traffic simulation. *Traffic engineering & control*, *35*(5), 317-321.

Gao, Y. (2008). Calibration and Comparison of the VISSIM and INTEGRATION Microscopic Traffic Simulation Models. *M.Sc. thesis, Virginia Polytechnic Institute and State University.*

Gartner, N., Messer, C. J., & Rathi, A. K. (2001). Traffic flow theory: A state-of-the art report. *Technical report, Transportation Research Board, USA.*

Gazis, D. C. (1967). Mathematical theory of automobile traffic. *Science, New series, 157*(3786), 273–281.

Gazis, D. C., Herman, R., & Rothery, R. W. (1961). Nonlinear follow-the-leader models of traffic flow. *Operations research*, *9*(4), 545-567.

Gipps, P. G. (1981). A behavioural car-following model for computer simulation. *Transportation Research Part B: Methodological*, *15*(2), 105-111.

Gipps, P. G. (1986). A model for the structure of lane-changing decisions. *Transportation Research Part B: Methodological*, *20*(5), 403-414.

Gomes, G., & Horowitz, R. (2006). Optimal freeway ramp metering using the asymmetric cell transmission model. *Transportation Research Part C: Emerging Technologies*, *14*(4), 244-262.

Gomes, G., May, A., & Horowitz, R. (2004). Congested freeway microsimulation model using VISSIM. *Transportation Research Record: Journal of the Transportation Research Board*, (1876), 71-81.

Greenberg, H. (1959). An analysis of traffic flow. *Operations research*, *7*(1), 78-85.

Greenshields, B. D. (1934). A study of traffic capacity. In *Highway Research Board Proceedings* Vol. 14, 448-481.

Gunay, B. (2007). Car following theory with lateral discomfort. *Transportation Research Part B: Methodological*, *41*(7), 722-735.

Gupta, A. K., & Khanna, S. K. (1986). Mixed traffic flow analysis for developing countries WST to India. In *Research for Tomorrow's Transport Requirements. Proceedings of the Fourth World Conference on Transport Research*, *Vancouver, Canada,* 1521–1534.

Hadiuzzaman, M., & Qiu, T. Z. (2013). Cell transmission model based variable speed limit control for freeways. *Canadian Journal of Civil Engineering*, *40*(1), 46-56.

Halkias, B., Kopelias, P., Papandreou, K., Politou, A., Prevedouros, P., & Skabardonis, A. (2007). Freeway Bottleneck Simulation, Implementation, and Evaluation. *Transportation Research Record: Journal of the Transportation Research Board*, *2012*(1), 84-93.

Hasan, M., Jha, M., & Ben-Akiva, M. (2002). Evaluation of ramp control algorithms using microscopic traffic simulation. *Transportation Research Part C: Emerging Technologies*, *10*(3), 229-256.

Hegyi, A., De Schutter, B., & Hellendoorn, H. (2005b). Model predictive control for optimal coordination of ramp metering and variable speed limits. *Transportation Research Part C: Emerging Technologies*, *13*(3), 185-209.

Hegyi, A., De Schutter, B., & Hellendoorn, J. (2005a). Optimal coordination of variable speed limits to suppress shock waves. *IEEE Transactions on Intelligent Transportation Systems, 6*(1), 102-112.

Herman, R., & Rothery, R. W. (1965). Car following and steady-state flow. In *Proceedings of the 2nd International Symposium on the Theory of Traffic Flow. Ed J. Almond, OECD, Paris*.

Hidas, P. (2002). Modelling lane changing and merging in microscopic traffic simulation. *Transportation Research Part C: Emerging Technologies*, *10*(5), 351-371.

Hoogendoorn, S. P., & Bovy, P. H. (2001). State-of-the-art of vehicular traffic flow modelling. *Proceedings of the Institution of Mechanical Engineers, Part I: Journal of Systems and Control Engineering*, *215*(4), 283-303.

Ishak, S., Alecsandru, C., & Seedah, D. (2006). Improvement and evaluation of cell-transmission model for operational analysis of traffic networks: freeway case study. *Transportation Research Record: Journal of the Transportation Research Board*, (1965), 171-182.

Islam, M., Hadiuzzaman, M., Fang, J., Qiu, T., & El-Basyouny, K. (2013). Assessing mobility and safety impacts of a variable speed limit control strategy. *Transportation Research Record: Journal of the Transportation Research Board*, (2364), 1-11.

Jin, S., Wang, D., Tao, P., & Li, P. (2010). Non-lane-based full velocity difference car following model. *Physica A: Statistical Mechanics and Its Applications*, *389*(21), 4654-4662.

Kerner, B. S., & Klenov, S. L. (2002). A microscopic model for phase transitions in traffic flow. *Journal of Physics A: Mathematical and General*, *35*(3), L31-L43.

Kerner, B. S., & Klenov, S. L. (2006). Deterministic microscopic three-phase traffic flow models. *Journal of Physics A: mathematical and general*, *39*(8), 1775-1809.

Khan, S., & Maini, P. (1999). Modeling heterogeneous traffic flow.*Transportation Research Record: Journal of the Transportation Research Board*, (1678), 234-241.

Kiefer, R. J., & Hankey, J. M. (2008). Lane change behavior with a side blind zone alert system. *Accident Analysis and Prevention, 40*(2), 683-690.

Kometani, E., & Sasaki, T. (1959). Dynamic behaviour of traffic with a nonlinear spacing–speed relationship. In *Proceedings of the Symposium on Theory of Traffic Flow, Research Laboratories, General Motors, New York: Elsevier*, 105-119.

Kotsialos, A., Papageorgiou, M., Diakaki, C., Pavlis, Y., & Middelham, F. (2002). Traffic flow modeling of large-scale motorway networks using the macroscopic modeling tool METANET. *IEEE Transactions on Intelligent Transportation Systems, 3*(4), 282-292.

Krauss, S., Nagel, K. & Wagner, P. (1999) The mechanism of flow breakdown in traffic flow models. In *Proceedings of the 14th International Symposium on Transportation and Traffic Theory (abbreviated presentations)*.

Lamon, F. (2008). Freeway traffic modelling and calibration for the Eindhoven network. *M.Sc. thesis, Delft University of Technology, The Netherlands*.

Lee, J. J., & Jones, J. H. (1967). Traffic dynamics: visual angle car following models. *Traffic Engineering & Control*, *8*(8), 348-350.

Leutzbach, W. (1988). *Introduction to the theory of traffic flow*. Berlin: Springer.

LeVeque, R. J., & Le Veque, R. J. (1992). *Numerical methods for conservation laws* (Vol. 132). Basel: Birkhäuser, Berlin.

Li, Z. (2010). Modeling arterial signal optimization with enhanced cell transmission formulations. *Journal of Transportation Engineering*, *137*(7), 445-454.

Lighthill, M. J., & Whitham, G. B. (1955). On kinematic waves. I. Flood movement in long rivers. II. A theory of traffic flow on long crowded roads. In *Proceedings of the Royal Society of London A: Mathematical, Physical and Engineering Sciences, 229*(1178), 281-345.

Lin, W. H., & Ahanotu, D. (1995). Validating the basic cell transmission model on a single freeway link. *PATH technical note; 95-3*.

Li-sheng, J., Wen-ping, F., Ying-nan, Z., Shuang-bin, Y., & Hai-jing, H. (2009). Research on safety lane change model of driver assistant system on highway. In *IEEE Intelligent Vehicles Symposium, Shaanxi, China,* 1051-1056.

Liu, G., Lyrintzis, A., & Michalopoulos, P. (1998). Improved high-order model for freeway traffic flow. *Transportation Research Record: Journal of the Transportation Research Board*, (1644), 37-46.

Lu, X. Y., Qiu, T. Z., Horowitz, R., Chow, A., & Shladover, S. (2011). METANET model improvement for traffic control. In *14th International IEEE Conference on Intelligent Transportation Systems, Washington, DC, USA,* 2148-2153.

Lu, X. Y., Qiu, T. Z., Varaiya, P., Horowitz, R., & Shladover, S. E. (2010). Combining variable speed limits with ramp metering for freeway traffic control. In *American Control Conference (ACC), 2010,* 2266-2271.

Lu, X. Y., Varaiya, P., Horowitz, R., Su, D., & Shladover, S. (2011). Novel freeway traffic control with variable speed limit and coordinated ramp metering. *Transportation Research Record: Journal of the Transportation Research Board*, (2229), 55-65.

Lygeros, J., Godbole, D. N., & Sastry, S. (1998). Verified Hybrid Controllers for Automated Vehicles. *IEEE Transactions on Automatic Control, 43*(4), 522-539.

Lyrintzis, A. S., Liu, G., & Michalopoulos, P. G. (1994). Development and comparative evaluation of high-order traffic flow models. *Transportation Research Record*, (1457), 174-183.

Messer, C. J. (1998). Simulation Studies of Traffic Operations at Oversaturated, Closely Spaced Signalized Intersections. *Transportation Research Record: Journal of the Transportation Research Board, 1646*(1), 115-123.

Messmer, A., & Papageorgiou, M. (1990). METANET: A macroscopic simulation program for motorway networks. *Traffic Engineering & Control*, *31*(8-9), 466-470.

Michaels, R. M. (1963). Perceptual factors in car following. In *Proceedings of the 2nd International Symposium on the Theory of Road Traffic Flow, Paris, France, OECD*, 44–59.

Michalopoulos, P. G., Yi, P., & Lyrintzis, A. S. (1992). Development of an improved high-order continuum traffic flow model. *Transportation Research Record*, (1365), 125-132.

Moridpour, S., Sarvi, M., & Rose, G. (2010). Lane changing models: a critical review. *Transportation letters*, *2*(3), 157-173.

Muñoz, L., Sun, X., Horowitz, R., & Alvarez, L. (2006). Piecewise-linearized cell transmission model and parameter calibration methodology. *Transportation Research Record: Journal of the Transportation Research Board*, (1965), 183-191.

Nair, R., Mahmassani, H. S., & Miller-Hooks, E. (2011). A porous flow approach to modeling heterogeneous traffic in disordered systems. *Transportation Research Part B: Methodological*, *45*(9), 1331-1345.

Newell, G. F. (1965). Instability in dense highway traffic, a review. In *Proceedings of the Second International Symposium on Transportation and Traffic Theory, London*, 73-83.

Olstam, J. J., & Tapani, A. (2004). *Comparison of Car-following models* (No. VTI report 960A).

Papageorgiou, M. (1990). Dynamic modeling, assignment, and route guidance in traffic networks. *Transportation Research Part B: Methodological*, *24*(6), 471-495.

Papageorgiou, M. (1998). Some remarks on macroscopic traffic flow modelling. *Transportation Research Part A: Policy and Practice 32*(5), 323-329.

Papageorgiou, M., Blosseville, J. M., & Hadj-Salem, H. (1989). Macroscopic modelling of traffic flow on the Boulevard Périphérique in Paris. *Transportation Research Part B: Methodological*, *23*(1), 29-47.

Papageorgiou, M., Blosseville, J. M., & Hadj-Salem, H. (1990). Modelling and real-time control of traffic flow on the southern part of Boulevard Peripherique in Paris: Part I: Modelling. *Transportation Research Part A: General*, *24*(5), 345-359.

Papamichail, I., Kotsialos, A., Margonis, I., & Papageorgiou, M. (2010). Coordinated ramp metering for freeway networks–A model-predictive hierarchical control approach. *Transportation Research Part C: Emerging Technologies*, *18*(3), 311-331.

Payne, H. J. (1971). Models of freeway traffic and control. *Mathematical models of public systems. (Simulation Council Proceedings),* Vol. 1, 51–61.

Payne, H. J. (1979). FREFLO: A macroscopic simulation model of freeway traffic. *Transportation Research Record*, (722), 68-77.

Pipes, L. A. (1953). An operational analysis of traffic dynamics. *Journal of applied physics*, *24*(3), 274-281.

PTV, AG. (2010, 2012). VISSIM 5.40 User Manual. *Karlsruhe, Germany*.

Richards, P. I. (1956). Shock waves on the highway. *Operations research 4*(1), 42-51.

Sanwal, K. K., Petty, K., Walrand, J., & Fawaz, Y. (1996). An extended macroscopic model for traffic flow. *Transportation Research Part B: Methodological*, *30*(1), 1-9.

Skabardonis A. (1999). Assessment of Traffic Simulation Models. *University of California, Berkley, Institute of Transportation Studies*.

Spiliopoulou, A., Kontorinaki, M., Papageorgiou, M., & Kopelias, P. (2014). Macroscopic traffic flow model validation at congested freeway off-ramp areas. *Transportation Research Part C: Emerging Technologies*, *41*, 18-29.

Stewart, J., Baker, M., & Van Aerde, M. (1996). Evaluating weaving section designs using INTEGRATION. *Transportation research record: Journal of the transportation research board*, (1555), 33-41.

Sukthankar, R., Baluja, S., & Hancock, J. (1997). Evolving an Intelligent Vehicle for Tactical Reasoning in Traffic. In *Proceedings of the International Conference on Robotics and Automation, New Mexico,* 519-524.

Todosiev, E. P., & Barbosa, L. C. (1964). A proposed model for the driver-vehicle system. *Traffic Engineering*, *34*(17), 17-20.

Toledo, T. (2007). Driving behaviour: models and challenges. *Transport Reviews*, *27*(1), 65-84.

Treiber, M., Kesting, A., & Helbing, D. (2010). Three-phase traffic theory and two-phase models with a fundamental diagram in the light of empirical stylized facts. *Transportation Research Part B: Methodological*, *44*(8), 983-1000.

Underwood, R. T. (1961). Speed, volume and density relationships: Quality and Theory of Traffic Flow, *Yale Bureau of Highway Traffic, New Haven, Conn.*, 141-188.

Van Aerde, M. (1995). Single regime speed-flow-density relationship for congested and uncongested highways. In *74th Annual Meeting of the Transportation Research Board, Washington, DC* (Vol. 6).

Van Aerde, M., & Rakha, H. (1995). Multivariate calibration of single regime speed-flow-density relationships. In *Proceedings of the 6th Vehicle Navigation and Information Systems Conference*, 334-341.

Venkatesan, K., Gowri, A., & Sivanandan, R. (2008). Development of microscopic simulation model for heterogeneous traffic using object oriented approach. *Transportmetrica*, *4*(3), 227-247.

Wiedemann, R. (1974). Simulation des Strassenverkehrsflusses. *University Karlsruhe, Germany*.

Wilson, R. E., & Ward, J. A. (2011). Car-following models: fifty years of linear stability analysis–a mathematical perspective. *Transportation Planning and Technology*, *34*(1), 3-18.

Wong, G. C. K., & Wong, S. C. (2002). A multi-class traffic flow model–an extension of LWR model with heterogeneous drivers. *Transportation Research Part A: Policy and Practice*, *36*(9), 827-841.

Wu, N. (2002). Application and verification of macroscopic and microscopic simulation models—case study for NETCELL and VISSIM on congested freeway. In *Proceedings of the International Conference on Traffic and Transportation Studies, Beijing, China*.

Yin, D. (2014). Traffic Flow Modelling to Improve Traffic State Prediction. *PhD dissertation, Department of Civil and Environmental Engineering, University of Alberta, Edmonton, Canada*.

Zhang, H. M. (1998). A theory of nonequilibrium traffic flow. *Transportation Research Part B: Methodological*, *32*(7), 485-498.

Zhang, H. M. (1999). A mathematical theory of traffic hysteresis. *Transportation Research Part B: Methodological*, *33*(1), 1-23.

Zhang, H. M. (2002). A non-equilibrium traffic model devoid of gas-like behavior. *Transportation Research Part B: Methodological*, *36*(3), 275-290.